Direct use of concrete tensile strength

Sustained Tensile Strength of Concrete

Résistance à la traction du béton sous charge de longue durée

Betonzugfestigkeit unter Dauerlast

Hisham SHKOUKANI
Civil Eng.
Technische Hochschule
Darmstadt, Germany

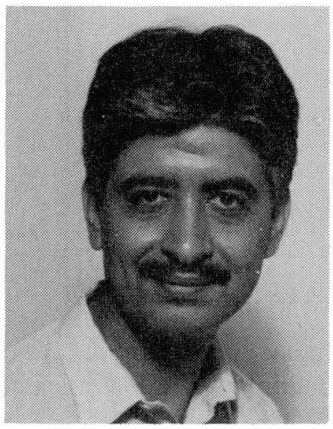

Hisham Shkoukani, born 1955, received his civil engineering degree at the Wayne State University, Detroit, Mich. In 1990 het received his Ph. D. at the TU Darmstadt.

Joost WALRAVEN
Prof. Dr.
Delft Univ. of Technol.
Delft, The Netherlands

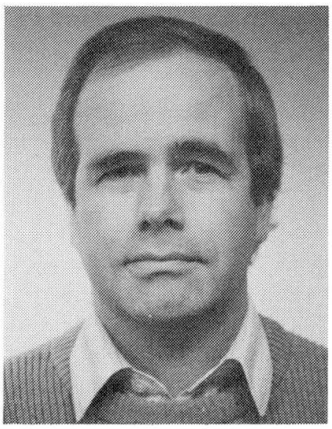

Joost Walraven, born in 1947, received his Ph. D. in Delft. After a period of consulting he became professor at the TU Darmstadt from 1985 – 1989, and at the TU Delft since 1989.

SUMMARY

Tests have been carried out in order to study the behaviour of concrete under concentric and eccentric sustained tensile loading. Variables were the eccentricity of the load, the shape of the concrete cross-section and the loading rate. Realistic values for the sustained tensile strength were determined, depending on the load level and the loading rate.

RÉSUMÉ

Des expériences ont été menées afin d'étudier le comportement du béton sous charge de traction centrée et excentrée. Les variables étudiées ont été l'excentricité de la charge, la forme de la section en béton et le temps de chargement; ceci aboutit à la détermination de la résistance à la traction, qui dépend du niveau de sollicitation et du temps de mise en charge.

ZUSAMMENFASSUNG

Es wurden Versuche zur Beschreibung des Verhaltens von Beton unter zentrischer und exzentrischer Dauerzugbeanspruchung durchgeführt. Dabei wurden unterschiedliche Exzentrizitäten sowie unterschiedliche Betonquerschnitte untersucht. Eine realistische Grösse der Zugfestigkeit des Betons unter Dauerbeanspruchung wurde in Abhängigkeit von Belastungsniveau und Belastungsgeschwindigkeit ermittelt.

1. INTRODUCTION

Nowadays the significant role of the tensile strength in the design of concrete structures begins to be reckognized. In the introductory lectures by Hillerborg and Duda/König many factors, influencing the concrete tensile strength and the post-cracking ductility, were discussed. However, hardly any attention has been devoted to the role of the so-called sustained loading effect. Nevertheless, if results of various authors may be believed, the sustained tensile strength is considerably lower than the tensile strength, obtained in a short term test. The ratio sustained to short term tensile strength is reported to be about 70%, see Fig. 1.

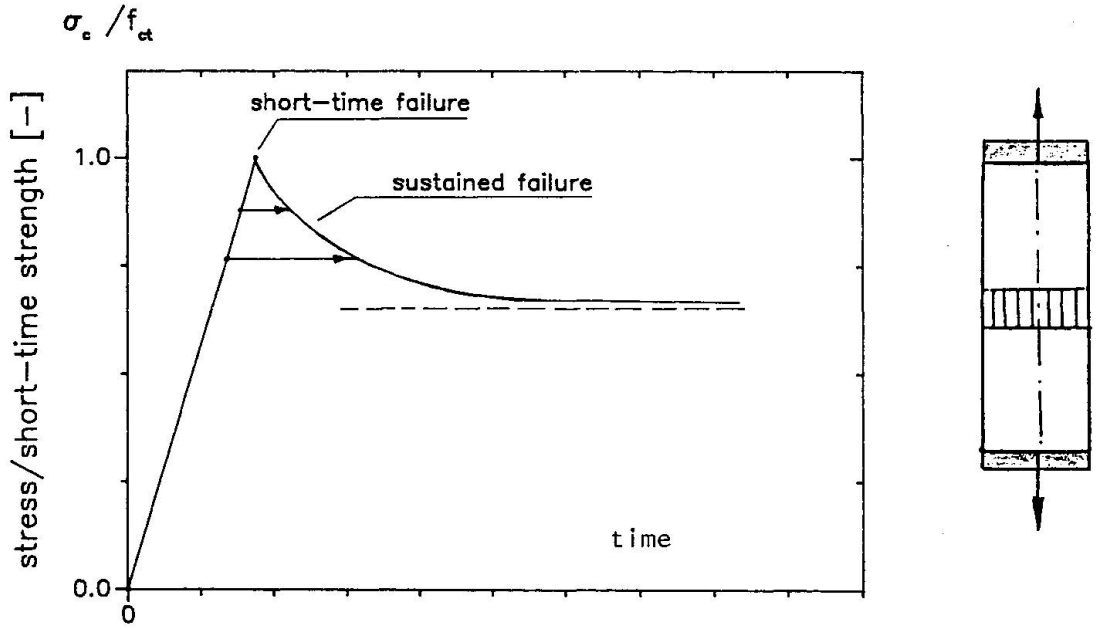

Fig. 1 Principle of sustained tensile test

An important observation is that this sustained strength-limit is reached after a relatively short period. A few days of sustained loading are sufficient to reach the 70% limit. This phenomenon may have important consequences, both in a favourable and in an unfavourable way. With regard to strength considerations, such as the shear capacity of members not reinforced in shear, a reduction of the capacity seems mandatory. On the other hand, a reduction of the tensile strength by sustained loading would have a positive effect in cases where minimum reinforcement is required due to the effect of imposed deformations. In this case the reduction of the tensile strength leads to a proportional reduction of the required amount of minimum reinforcement.

This shows that it is worthwhile to consider the influence of the strain rate more in detail. A number of questions can be raised, f.i.

- To what extend does the sustained strength-limit depend on the definition of the short term tensile strength? If the loading rate of the short-term test is not the same in all the tests, the sustained strength-limits $f_{ct,\infty}/f_{ct,o}$ as reported by various authors in the literature, are not comparable.
- Up to now only concentric sustained tensile tests have been reported. Many structural actions, however, lead to stress gradients. It is questionable if the results of concentric tensile tests can be applied to eccentric load application, or to flexure.
- Furthermore it may be wondered if the classical sustained loading test is representative for any loading case. If imposed deformations are concerned, the tensile stresses develop slowly in time and reach the cracking level within a period which may vary between hours and days.

In order to generate answers on these questions a number of tests has been carried out.

2. EXPERIMENTS

2.1 Sustained concentric tensile loading tests

The classical concept of a sustained loading test is as follows. The short term tensile strength (rapid test) is determined with a certain loading rate: subsequently, concrete with the same properties and storage conditions are loaded to a certain fractile of the previously determined short-term tensile strength. At this loading level the stress is kept constant. For high levels ($\frac{\sigma_c}{f_{ct}} > 0,7$), the concrete is observed to fail after a certain period.
This principle of testing was adopted for the first series of tests. The tests were carried out on cylindrical (ϕ 150 x 300 mm) and rectangular (150 x 150 x 300 mm) specimens, casted vertically in steel moulds. In order to prevent the development of internal stresses by shrinkage, the specimens were sealed before and during testing with plastic sheets. The average cube strength was 32 N/mm^2.

The short-term tensile strength was determined by testing specimens with such a loading rate that failure occured after about 10 seconds. In the sustained loading tests, the sustained load level was reached within one minute. Then the load was kept constant until failure occurred. The results of these tests are shown in Fig. 2.

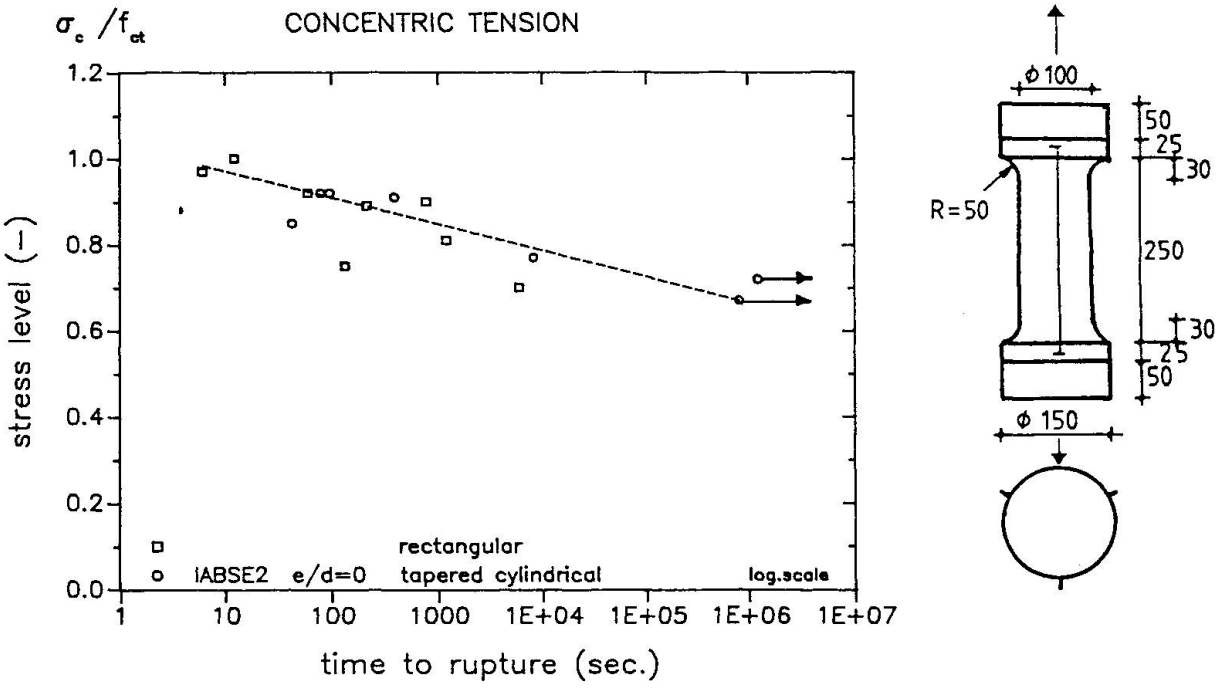

Fig. 2 Relationship between relative sustained stress level and time to failure for the concentric tensile tests

It can be seen that time to rupture increases with decreasing stress level σ_c/f_{ct}. It was found that, if a specimen did not fail within the first three hours, no failure at all occurred (the maximum loading time was two weeks). The lower limit of σ_c/f_{ct}, as observed, was 0.7. The specimens which did not fail after a period of sustained loading were subsequently loaded to failure in a rapid tests. Surprisingly, the strength obtained after this procedure was significantly higher than the strength obtained in a short term test on virgin specimens! This cannot be explained by the effect of continuing hydration, since an increase in strength was also observed after a sustained load of only a few hours. This might be explained by relaxation of the cement matrix during sustained loading, which could lead to a relaxation of stresses at the tip of the micro-cracks.

2.2 Sustained eccentric tensile loading tests

After the concentric tensile loading tests, a series of experiments was carried out on specimens, subjected to an eccentric tensile load. The relative load-eccentricities adopted in

the tests were e/d = 0.167 and 0.5.

Figs. 3a and b show, that the decrease of the strength by sustained loading, is smaller, the larger is the eccentricity of the load. For e/d = 0.167 no failure was observed to values of σ_c/f_{ct} smaller than 0.75. For e/d = 0.50 the lower limit was even about 0.9.

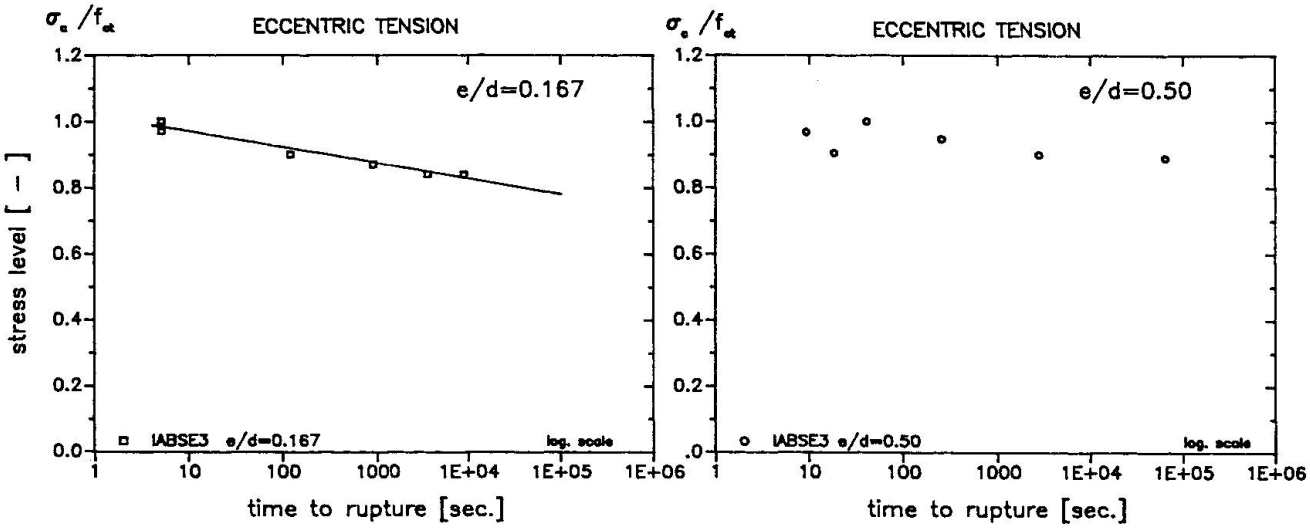

Fig. 3 Relation between relative stress level and time to rupture by eccentric tensile loading, with e/d = 0.167 and e/d = 0.50.

Also here the specimens which did not fail during sustained loading where loaded to failure in a short term test, and also here an increase of the strength was observed.

Obviously the sustained loading effect consists of two mechanisms, a damaging one and a hardening one. If the damaging mechanism is not strong enough to cause failure, the hardening mechanism starts to dominate, which results in a higher strength than the original one.

2.3 Eccentric tensile tests with different loading rates

If the previous conclusions, concerning damaging and hardening, were true, this would mean that, in case of a constant loading rate, a reduction of this loading rate could possibly lead to an increase of the strength. In order to examine this phenomenon, cylindrical specimens were loaded up to failure with different loading rates. The failure occurred after about 6 seconds, 2 minutes, 20 minutes, 1 hour and 2,5 hours. Fig. 4 shows the relationship between the failure load after the loading rate.

In Fig. 4 the loading rate is represented along the horizontal axis. The highest loading rate was such, that failure occurred in about 6 seconds (righthand side of the diagram). If the loading rate is decreased (passing from right to left), the strength decreases too. However, further lowering the loading rate leads to an increase of the strength.

This is remarkable because in such a situation, which reflects f.i. the case of stresses by imposed deformations (such as solar radiation), the lowest strength is obtained for a loading rate, which is generally considered as belonging to a short term test. Tensile splitting tests, carried out on control specimens, as usual in practice, do generally not require more than 2 minutes, so that application of a strength reduction factor to consider a sustained loading effect in practical situations seems to be unjustified.

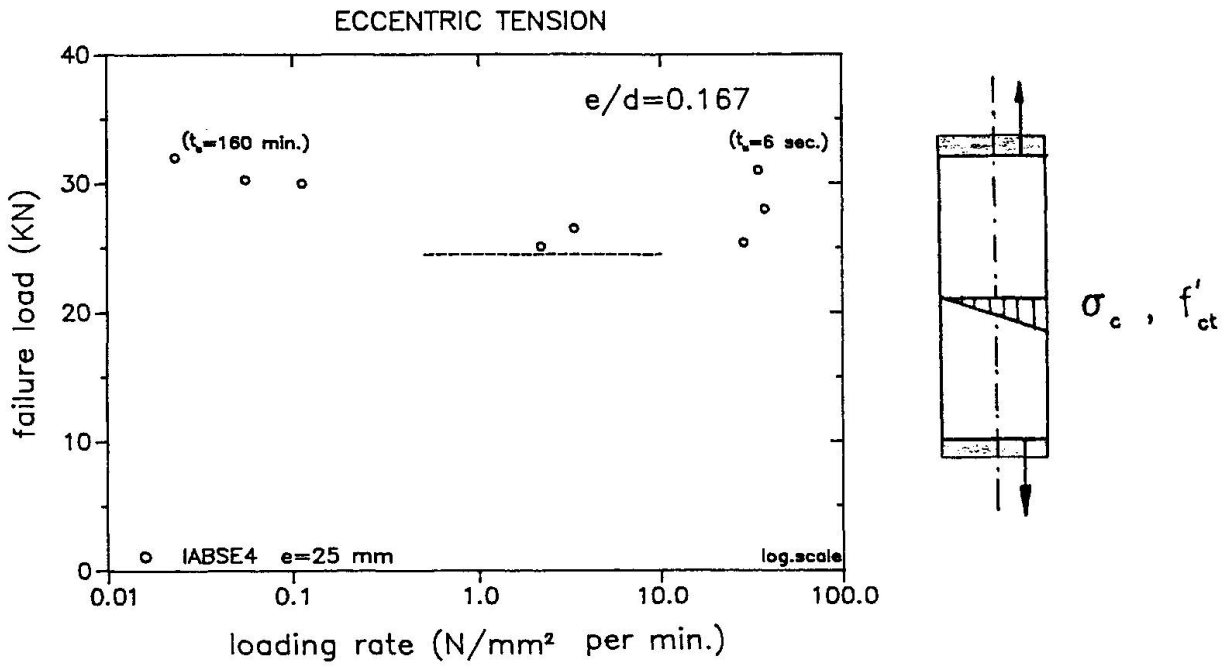

Fig. 4 Relationship between failure tensile load and loading rate for an eccentricity of e/d = 0.167

3. CONCLUSIONS

- In concentric tensile tests the strength under sustained loading is smaller than under short-term loading. In order to determine the sustained strength limit, a clear definition of the short-term strength is necessary. If the short-term strength is determined within a failure time of 10 seconds, the sustained tensile strength is about 70% of the short-term strength, whereas in the case of 100 seconds failure time, the sustained tensile strength is about 85% of the short-term strength.
- The sustained tensile strength increases with increasing eccentricity: i.e. if a stress gradient is available over a cross-section, and the short term strength is defined as that strength, which is obtained in 100 seconds, the sustained loading effect can be neglected.
- In addition to the damaging effect there is also a hardening effect, which can probably be explained by the reduction of the peak stresses by relaxation. This is most effective if the loading rate is relatively small.

REFERENCES

1. Reinhardt, H.W., Cornelissen, H.A.W., Sustained Tensile Tests on Concrete. Baustoffe '85, Bauverlag, Wiesbaden, 1985, pp. 162-167.
2. Shkoukani, H., Beton unter Dauerzugbeanspruchung. Tagungsband zum Darmstädter Massivbau-Seminar, Band 1, Rissbreitenbeschränkung und Mindestbewehrung, THD, 1989.

Leere Seite
Blank page
Page vide

Use of the Tensile Strength in Anchorage to Concrete

Emploi de la résistance à la traction lors d'ancrages dans le béton

Rechnerische Erfassung der Bauteilbeanspruchungen durch Befestigungen

Rolf ELIGEHAUSEN
Prof. Dr.
Univ. Stuttgart
Stuttgart, Germany

Rolf Eligehausen, born 1942, received his Dipl. Ing. in 1968 at the Technical University Braunschweig and Dr. Ing. in 1979 at the University of Stuttgart. From 1979 – 1981 he was research engineer at the University of California at Berkeley. Since 1984 he is Professor for fastening technology at the Institute für Werkstoffe im Bauwesen, Stuttgart.

Josko OZBOLT
Dr. Ing.
Univ. Stuttgart
Stuttgart, Germany

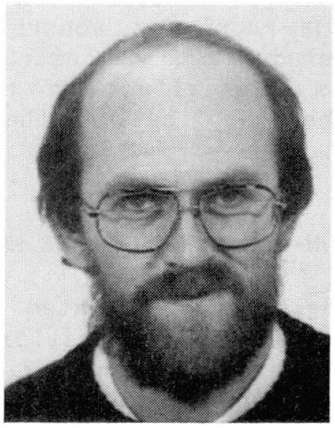

Josko Ozbolt, born 1955, received his Dipl. Ing. in 1978 and Dr. Ing. in 1982 at the University of Zagreb. In 1980 he performed a post-graduate study at the TNO Institute in Delft, and from 1987 – 1988 a postdoctoral study at Northwestern University. Since 1989 Research Engineer at Institut für Werkstoffe im Bauwesen, Stuttgart.

SUMMARY

Anchoring elements, such as headed studs, are used to transfer concentrated loads into reinforced concrete members. From experimental evidence it is known that, provided the steel strength of the stud is high enough, failure occurs by pulling out a concrete cone formed by circumferential crack growth in the so-called mixed mode, with significant size effect. Numerical analyses indicate that the dominant influence factor on the failure load is the concrete fracture energy. It is shown that in such applications, the load transfer from the anchor into the concrete may safely be done by using the concrete tensile strength.

RÉSUMÉ

Des éléments d'ancrage tels que les boulons sont utilisés pour transmettre localement des charges dans une structure en béton armé. Selon l'évidence expérimentale, il est clair que si la résistance de l'acier du boulon est suffisante, la ruine est atteinte par arrachement d'un cône en béton: une fissure circulaire se développe, accompagnée d'un effet de taille significatif dans ce qu'on appelle un «mode mixte». Les analyses numériques indiquent que l'influence dominante sur la charge ultime a l'énergie de fracture du béton. Il est très intéressant que dans ce type de structures, le béton puisse transmettre des charges de l'ancrage à la masse enserrante sans l'aide de l'armature, et ceci grace à la mobilisation de sa résistance à la traction.

ZUSAMMENFASSUNG

Befestigungselemente wie Kopfbolzen werden häufig eingesetzt, um Lasten in Stahlbetontragwerke einzuleiten. Versuche zeigen, dass das Versagen bei ausreichend hoher Stahltragfähigkeit durch die Ausbildung eines Betonausbruchkegels hervorgerufen wird. Die Bruchlast hängt nach den Ergebnissen der numerischen Untersuchungen hauptsächlich von der Betonbruchenergie ab. Es wird diskutiert, dass in diesen Anwendungsfällen die Betonzugfestigkeit in Anspruch genommen werden kann, ohne dass ein Sicherheitsrisiko besteht.

1. INTRODUCTION

In engineering practice, headed anchors are often used to transfer loads into concrete structures. From experimental evidence it is known that, provided the steel strength of the anchor is high enough, headed anchors fail by pulling a concrete cone. The failure is due to the failure of concrete in tension by forming a circumferential crack growing in the so-called mixed mode [1]. In recent years several attempts have been made to understand this growth and to predict the failure load of headed studs [1] - [4]. Summarizing these activities, it can be said that material models based on plasticity and on stress-strain relationships together with stress failure criteria are not capable of predicting the behavior of anchors as observed in experiments [1], [5]. Furthermore, the predicted failure load depends on the element size and load step size. A better explanation of anchorage behavior can be expected using more general material models based on fracture mechanics. Some recent results of the numerical analysis using axissymmetric finite elements and a non-local microplane model for concrete are shown and discussed. The main objective of this study is to demonstrate the influence of different concrete properties and the size effect on the failure load. Furthermore, it is discussed why in these applications the concrete tensile strength can be used without safety risk.

2. REVIEW OF THE NON-LOCAL MICROPLANE MODEL

The microplane models were initiated by G.I.Taylor [6], who suggested the principle for the modeling of plasticity of polycrystaline metals. Recently [7], this approach has been extended to include strain softening of concrete, and has been renamed more generally the "microplane model", in recognition of the fact that the approach is not limited to plastic slip but can equally well describe cracking and strain softening damage.
Basically, on the material level one may distinguish two types of interactions among particles or damage sites in the microstructures, which must be somehow manifested in the continuum model: (1) Interaction at a **distance** among various sites (e.g., between A and B, in Fig. 1); and (2) interaction **among various orientations** (see angle α in Fig. 1).
The interactions at a distance control the localization of damage. They are ignored in the classical, local continuum models, but are reflected in non-local models [8]. According to the non-local strain concept, the stress at a point depends not only on the strain at that point but also on the strain field within a certain region around the point. In the current study, an effective form of the non-local concept is used in which all variables that are associated with strain softening are non-local and all other variables are local [9]. The key parameter in the non-local concept employed is the characteristic length l_c over which the strains are averaged. However, it is still not clear how to correlate the characteristic length with concrete properties in general 3D stress-strain states. In a preceding paper [9] the non-local microplane model as well as an effective numerical iterative algorithm for the loading steps used in the finite element code are described in detail.

3. REVIEW OF THE NUMERICAL STUDIES ON THE BEHAVIOR OF ANCHORAGES

The behavior of headed studs embedded in reinforced concrete blocks is studied in [10] - [12]. In these studies, the influence of the different material and geometrical parameters on the concrete cone failure is investigated. The concrete
tensile and compression strength, fracture energy, initial Young's modulus and

the size of the stud are varied. To demonstrate the size effect, the influence of the embedment depth on the failure load is studied.
The analysis is performed using axissymmetric four-node finite elements and the non-local microplane model. A typical finite element mesh employed in the analysis is shown in Fig. 2. Fig. 3 shows a comparison between test results and results of the numerical analysis and demonstrates that the non-local microplane model can correctly predict the concrete cone failure load.
Fig. 4 demonstrates the influence of the concrete fracture energy G_F on the failure load. In these studies, the concrete tensile strength was kept constant. According to the Fig. 4, the failure load is roughly proportional to the square root of G_F. The influence of the tensile strength, for a constant value of G_F, on failure load is shown in Fig. 5. It indicates that the concrete tensile strength has a small influence on the concrete cone failure load. Both results are also confirmed by Sawade [5]. Concrete compression strength and the size of the head have a significant influence on the displacement field, but a relatively little influence on the failure load [11].
Because the analysis shows the dominant role of the concrete fracture energy on the anchor behavior a large size effect on the failure load must be expected. Indeed, results of numerical analyses obtained in [11] and [12], as well as test results indicate a significant size effect that is close to that predicted by linear elastic fracture mechanics (Fig.6).
In spite of the fact that the G_F value has a dominant influence on the concrete cone failure load, the design of fastenings should be based on the concrete compression strength, since this concrete property can easily be measured and is known to the designer.

4. USE OF THE TENSILE STRENGTH IN ANCHORAGES

In many applications, no reinforcement can be provided in the region of headed anchors that could take up the load transferred by the anchor into the structure. Therefore, these forces must be resisted by the concrete tensile strength. In contrast to that, generally in reinforced concrete design, the concrete tensile strength is neglected and any tensile stresses in the concrete are taken up by reinforcement. This approach is justified by the fact that tensile stresses may be induced in the concrete by the restraint of imposed deformations i.e. due to creep, shrinkage, temperature variations or support settlements, which may reach the concrete tensile strength and cause cracks in the concrete. These stresses are parallel to the tension stresses (i.e. bending stresses) induced by loads. Therefore, failure of the structure may be caused by the restraint of imposed deformations if no reinforcement is present to take up the tensile forces due to loads.
In the case of headed studs embedded in concrete, the situation is somewhat different. The failure surface is not perpendicular to the load directions and the tensile stresses on the failure plane are inclined to the concrete surface (Fig. 7). Therefore, the tensile stresses induced by the anchor load intersect with additional tensile stresses generated in the concrete and due to the restraint of imposed deformations, which are parallel to the concrete surface over a small part of the failure area only. Furthermore, the fracture process is very stable up to peak load because the circumferential crack forms a cone and the crack tip has to penetrate a larger area the move it grows. Therefore, if the additional stresses cause locally the formation or widening of a microcrack, stable stress redistribution is possible. According to rough theoretical investigations a reduction of the concrete cone failure load by about 20% can be expected if the additional tensile stresses σ_{add} reach the concrete tensile strength [13]. This possible reduction of the failure load is smaller than the reduction which must be expected if the anchor is located in a crack [14]. It should be taken into account in the design of the

fastening. Naturally, reinforcement must be present to prevent failure of the structure serving as anchor ground.

5. CONCLUSIONS

The numerical results as well as experimental observations indicate that the failure of headed studs embedded in plain concrete is due to failure of concrete in tension (circumferential cracking) rather than in compression. The failure load is mainly influenced by the concrete fracture energy G_F. However, the design of fastenings should be based on the concrete compression strength, since that value is known to the designer.
In spite of the fact that the concrete cone failure load is governed by the tensile properties of concrete, no reinforcement is necessary to take up the concrete tensile stresses induced by the anchor. This can be explained by the fact that the tensile stresses induced in the concrete by other external loads or by restraint of imposed deformations , e.g. due to temperature variations, intersect hardly with the tensile stresses induced by the anchor. Furthermore, the fracture process is very stable so that a stable stress redistribution is possible if local cracks are caused in the concrete by these additional tensile stresses. However, reinforcement may be provided to increase the anchor strength.

6. REFERENCES

1. ELIGEHAUSEN, R. and SAWADE, G. - 'Analysis of Anchoring Behavior (Literature Review)', Fracture Mechanics of Concrete Structures - RILEM Report, Ed. L.Elfgren, Chapman and Hall, 1989, pp.263-280.

2. OTTOSEN, N. S. - Nonlinear Finite Element Analysis of Pull-Out Tests. Journal of Structural Division, Vol. 107, No. ST4, pp. 591-603, 1981.

3. ELIGEHAUSEN, R. and SAWADE, G. - Behavior of Concrete in Tension. Betonwerk + Fertigteil Technik, No. 5 and 6, 1985.

4. KRENCHEL, H. and SHAH, S. - Fracture Analysis of the Pull-Out Tests. Material and Structures, Vol. 18, No. 108, pp. 439-446, 1985.

5. SAWADE, G. - Ein Beitrag zum Verhalten von zugbeanspruchtem Beton (A contribution to the behavior of concrete in tension). Thesis in preparation, Stuttgart University, in German.

6. TAYLOR, G.I., Plastic strain in metals. J. of Inst. of Metals, 62, 1983, pp. 307-324.

7. BAZANT, Z.P., and PRAT, P.C., Microplane model for brittle-plastic material - parts I and II. J. of Eng. Mech., ASCE, 114 (10), 1988, pp. 1672-1702.

8. BAZANT, Z.P., and PIJAUDIER-CABOT, G., Nonlocal continuum damage, localization instability and convergence. J. of Appl. Mech., ASME, 55, 1988, pp. 287-293.

9. BAZANT, Z.P., and OZBOLT, J., Nonlocal microplane model for fracture, damage and size effect in structures. J. of Eng. Mech., ASCE, 116, (11), 1990, pp. 2485-2505.

10. OZBOLT, J. and ELIGEHAUSEN, R., Numerical Analysis Of Headed Studs Embedded in Large Plain Concrete Blocks, Proceedings of the 2nd International Conference of Computer Aided Analysis and Design of Concrete Structures, Zell am See, Austria, April 1990, pp. 465 - 656.

11. OZBOLT, J. and ELIGEHAUSEN, R., Numerical Analysis of Headed Studs Embedded in Large Plain Concrete Blocks, Report Nr. 4/10 - 90/9, IWB, Stuttgart University, Oct. 1990.

12. ELIGEHAUSEN, R. and OZBOLT, J., Size effect in Anchorage Behavior, Proceedings of the Eight European Conference on Fracture - Fracture Behavior and Design of Materials and Structures, Torino, Italy, 1-5 October 1990.

13. Rehm, G., Eligehausen, R. and Silva, J., Dübel in der aus Lastspannungen erzeugten Zugzone von Stahlbetonbauteilen. Report No. 1/1-82/1 of the Institut für Werkstoffe im Bauwesen, Universität Stuttgart, June 1982.

14. Rehm, G., Eligehausen, R. and Mallie, R., Befestigungstechnik, Betonkalender 1988, Teil 2, Wiehelm Ernst & Sohn, berlin, 1988.

7. FIGURES

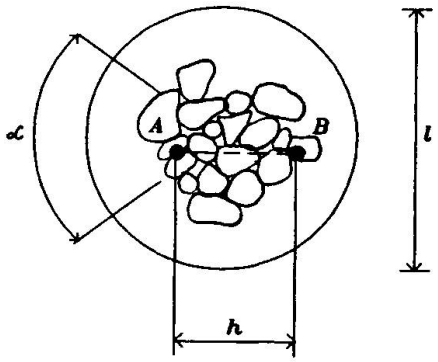

Fig. 1 Interaction among the various orientations and at distance

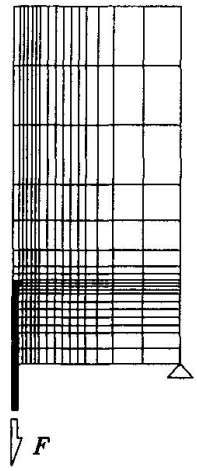

Fig. 2 Typical finite element mesh used in the analysis

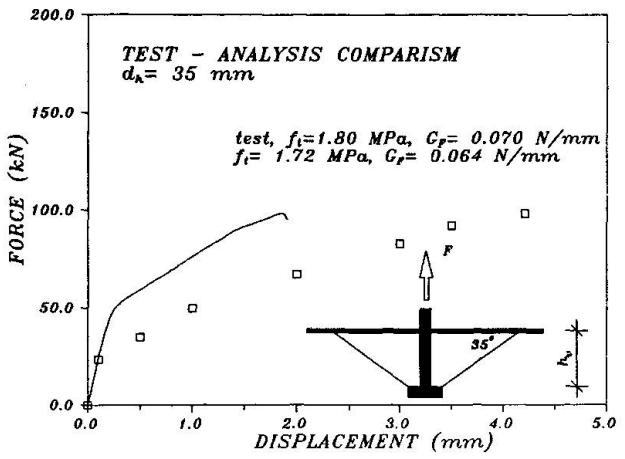

Fig. 3 Experiment-analysis comparison

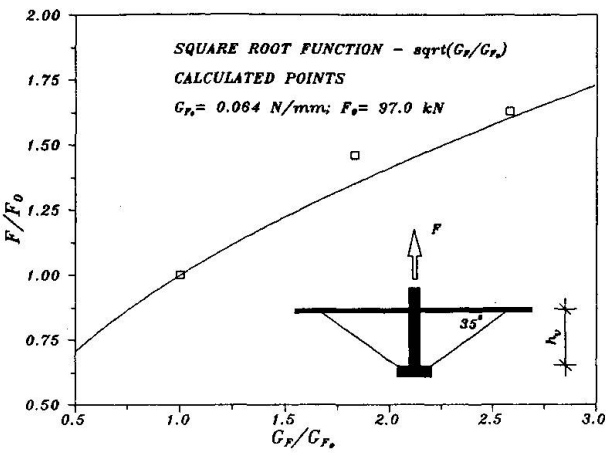

Fig. 4 Influence of the fracture energy on the failure load

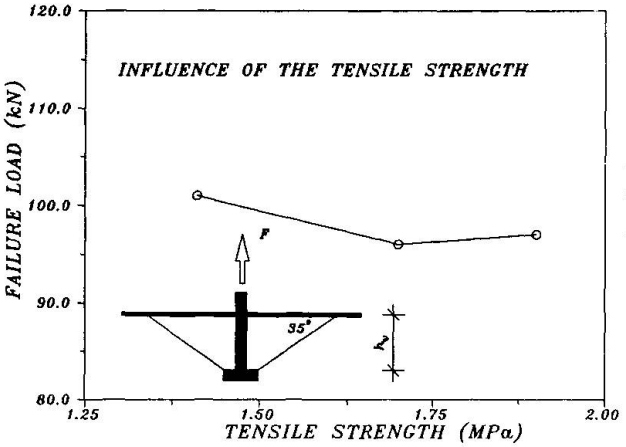

Fig. 5 Influence of the tensile strength on the failure load

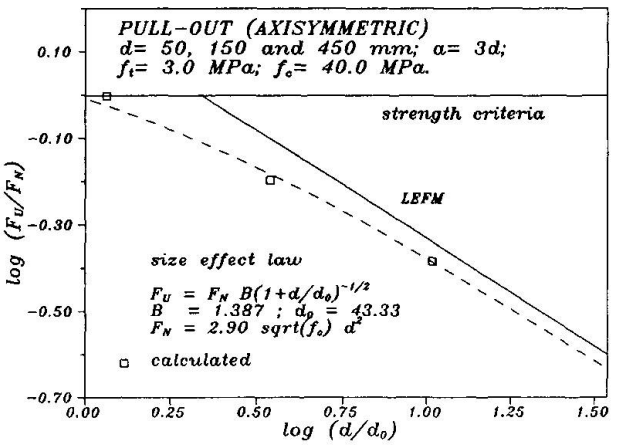

Fig. 6 Size effect on the pull-out load

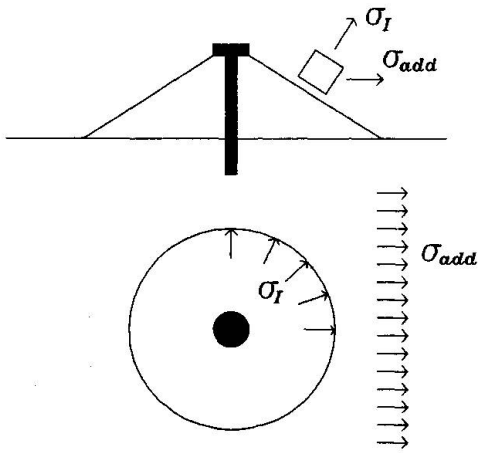

Fig. 7 3D stress state along the concrete cone failure surface and additional tensile stresses

Numerical Analysis of Anchoring Effects in Structures

Analyse numérique des effets d'ancrage dans les structures

Nutzung der Betonzugfestigkeit in der Befestigungstechnik

Rolf ELIGEHAUSEN
Prof. Dr.
Univ. Stuttgart
Stuttgart, Germany

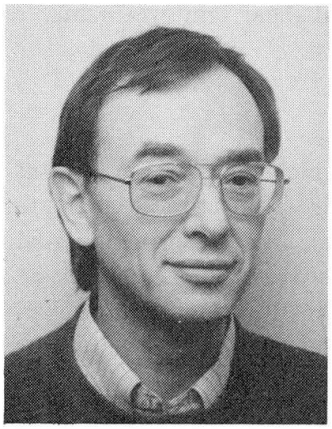

Rolf Eligehausen, born 1942, received his Dr. Ing. in 1979 at Univ. of Stuttgart. 1979 – 1981 Research Engineer at Univ. of California at Berkeley. Since 1984 Professor for fastening technology at the Inst. für Werkstoffe im Bauwesen, University Stuttgart.

Mihajlo KAZIC
Res. Eng.
Univ. Stuttgart
Stuttgart, Germany

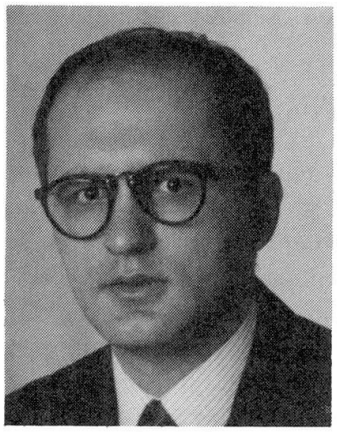

Mihajlo Kazic, born 1960, obtained his B.S. degree in 1983 in Novi Sad YU, M.S. and Ph.D. in 1986 and 1988 at Univ. of California Los Angeles. Senior Consultant at Pavlovich & Assoc. in L.A. and Teaching Assoc. at UCLA. Since 1989 Research Eng. at IWB, University Stuttgart.

SUMMARY

The shear behaviour of reinforced concrete beams with various types of vertical shear reinforcements and for different load arrangements, modelling the action of headed anchors installed in the tension zone, is numerically analysed by a non-linear finite element program based on a smeared crack approach taking into account non-linear fracture mechanics. Factors affecting the ultimate shear strength are discussed with respect to the numerical analysis and the overall structural response.

RÉSUMÉ

Le modèle mécanique d'affaiblissement de contrainte après fissuration du béton en traction, ainsi que la résistance-même en traction de ce matériau constituent le base du modèle de discrétisation des fissures dans une analyse par éléments finis. Ce concept est ultilisé dans l'analyse du problème du cisaillement de poutres en béton armé sous différentes positions de la charge, celle-ci cheminant dans la matière au moyen des éléments d'armature ancrés dans le béton et les étriers. Les facteurs qui influent sur la résistance ultime à l'effort tranchant sont discutés à la lumière du respect des dispositions énoncées par la Norme au sujet des techniques d'ancrage.

ZUSAMMENFASSUNG

Es wird der Einfluss von durch Kopfbolzen in die Betonzugzone eingeleiteten Lasten auf das Schubtragverhalten von Stahlbetonbalken mit unterschiedlichen Schubbewehrungen untersucht. Die Studien werden mit einem nichtlinearen FE-Programm durchgeführt, das auf dem Konzept der verschmierten Risse unter Berücksichtigung der nichtlinearen Bruchmechanik beruht. Die das Schubtragverhalten beeinflussenden Faktoren werden diskutiert.

1. INTRODUCTION

The shear strength of reinforced concrete beams is almost exclusively studied for the cases where the loads are applied through plates directly onto the top beam surface. However, in modern structures the loads may partly be applied by means of high-tech metal anchoring elements placed in the bottom part of the beam. The influence of this load application by means of anchoring elements on the shear strength of beams without shear reinforcement has been extensively studied by Eligehausen et al. [3]. Their principal conclusion was that on an average the shear failure load is reduced by 10% when the entire load is applied by means of anchoring elements placed in the bottom, tensile zone. The same conclusion was verified by Cervenka et al. [2] in a finite element analysis of reinforced concrete beams with no shear reinforcement.

The present analysis is accomplished by the FE program AXIS, developed at the Institut für Werkstoffe im Bauwesen, University of Stuttgart. The goal was to study the influence of loads introduced into the bottom zone on the shear strength of beams with different vertical shear reinforcements.

2. SCOPE OF ANALYSIS

The analysis concerns reinforced concrete beams failing in shear. The dimensions of the T-beam (Fig. 1) and the shear span ratio $\lambda = a/d = 2.8$ are chosen in order to ensure a shear-tension failure and to avoid a shear-compression (for small λ) and bending failure (for large λ). The principal goal is to investigate the influence of different load arrangements for various stirrups cross-sections on the shear strength. Three different loading cases may be distinguished from Fig. 2, in which load case *a* represents a beam with concentrated loads applied on the top surface. Load case *b* represents the application of 20% of the total loads by means of anchoring elements placed in the bottom zone. Load case *c* is analysed for the sake of direct comparison with load case *b*, with the same shear span ratio and load proportions, but with loads placed on the top surface. Each of this three loading cases was applied on a beam with five different stirrups configurations (no stirrups; two-legged $\phi 6$, $\phi 8$, $\phi 10$ and four-legged $\phi 8$ stirrups, each at a spacing $s = 0.15m$). The longitudinal reinforcement ratio $\rho_w = 2.38\%$ is taken as constant in order to preclude the influence of its variability on the results. Yielding point for all stirrups is $f_{sy} = 350MPa$ and for bending reinforcement $f_y = 450MPa$.

In the bottom part of the web, headed studs with anchoring length $h_v = 100mm$ are located. The stud spacing $s = 0.30m$ is chosen in order to avoid mutual effects of neighbouring studs [3]. The loads applied on the studs are proportional to the loads applied on the top surface, and are smaller than the concrete cone failure load of $55.0kN$ (according to [3]).

Only the effects of static loading are considered. The loads are increased gradually. Load increments are not equal, and depend on the employed arc length iterative procedure, which is a displacement controlled analysis. Effects of repeated, dynamic or reversed loading were not studied.

3. FE ANALYSIS: MATERIAL MODEL

3.1 Concrete Parameters

Reinforced concrete is a highly nonlinear structural material. Prior to crushing or tensile failure, in the FE program AXIS, concrete is considered as a hyperelastic material, for which the stress-strain relations are of the form:

$$\sigma_{ij} = F(I_1, J_2, J_3)\epsilon_{ij} \tag{1}$$

where the initial elastic constants are replaced by scalar functions $F(I_1, J_2, J_3)$ associated with the first invariant I_1 of the stress tensor and the second and third invariants J_2, J_3 of the deviatoric

stress tensor. The nonlinear isotropic elastic stress-strain relation prior to crushing or tensile failure is modelled by a quadratic parabola in compression and by linear loading in tension. A linear strain softening is assumed after crushing and after tensile failure (Fig. 3). The scalar functions $F(I_1, J_2, J_3)$, developed from Kupfer's biaxial experimental data are established to include the variable peak strengths in compression or tension, depending on the total state of stress. The crack is initiated after the principal stress exceeds the tensile strength. The softening modulus in tension E_T is based on nonlinear fracture mechanics and calculated according to the crack band theory of Bazant and Oh [1] :

$$E_T = \frac{E}{1 - \frac{L_{ch}}{L_e}} \qquad L_{ch} = \frac{2G_f E}{f_{ct}^2} \tag{2}$$

in which L_e is the width of an element, or the square root of the area assigned to an integration point. The value L_{ch}, called characteristic length is assumed to be a material property dependant on the fracture energy G_f, modulus of elasticity E and the direct tensile strength f_{ct}.

In the present analysis, the material properties are characterized by only three material parameters, with the following values: uniaxial compressive strength $f_c = 30MPa$, Poisson ratio $\nu = 0.17$ and fracture energy $G_f = 66N/m$. The direct tensile strength f_{ct} is assumed to be a function of the compressive strength:

$$f_{ct} = 0.269 f_c^{0.666} \implies f_{ct} = 0.269(30.0)^{0.666} = 2.60MPa \tag{3}$$

The values of the initial tangent modulus and softening modulus in compression are assumed as:

$$E = 5015\sqrt{f_c} \quad [MPa] \implies E = 27500MPa \tag{4}$$

$$E_{cc} = -E_c/8.0 \implies E_{cc} = -3500MPa \tag{5}$$

3.2 Shear transfer across the crack

Employing a smeared crack approach, the FE program AXIS has the options for both the fixed crack model based on orthotropic concepts and the rotating crack model based on nonlinear elasticity relations in principal coordinates. In the fixed crack model, the mechanisms of shear transfer accross the crack due to aggregate interlock or dowel action is simulated by reducing the value of the shear modulus corresponding to the crack plane according to the following expression:

$$G = \beta G_{initial} = \beta \frac{E}{2(1+\nu)} \tag{6}$$

In the program, the shear retention factor β can be assumed as constant or variable. For a variable β value the following expression derived by Kolmar [5] is utilised:

$$\beta = -\frac{ln\frac{\epsilon_m}{c_1}}{c_2} \qquad c_1 = 7.0 + 5.0\left(\frac{\mu - 0.005}{0.015}\right) \qquad c_2 = 10.0 - 2.5\left(\frac{\mu - 0.005}{0.015}\right) \tag{7}$$

in which ϵ_m (given in $^o/_{oo}$) is the strain perpendicular to the crack and $\mu \leq 0.02$ is the reinforcement ratio related to the considered finite element.

4. RESULTS OF THE NUMERICAL ANALYSIS

The influence of different crack models on the load displacement behavior of one analysed beam (load case a, stirrups $\phi 10$) is shown in Fig. 4. When using a fixed crack model in connection with variable shear retention factor according to Eq. 7, the beam fails in shear. However, the use of a fixed crack

model with constant shear retention factor, or a rotating crack model will result in a completely different behavior, namely a bending failure with considerably higher ultimate loads. Therefore, the fixed crack model with shear retention factor by Kolmar is used for the entire analysis.

The ultimate stage is reached after extensive diagonal cracking and after yielding of stirrups in case of beams with shear reinforcement. The ultimate shear forces P_u for all analysed cases are listed in Table 1. The ultimate shear stresses, computed by $v_u = P_u/(7bd/8)$, are shown in Fig. 5. A comparison of the results for load case a with empirical formulas by Kordina and Blume [6], Mallèe [7] and Specht [8] is presented in Fig. 6 (see [4] for details). For lower shear reinforcement ratios, the FE analysis gives higher ultimate shear stresses than the empirical formulas. This can be explained by the fact that with the FE analysis a T-beam was considered, while the empirical formulas are valid for beams with rectangular cross section. Test results prove that the shear strength of T-beams is about 20% higher than for beams with rectangular cross-section. Numerically obtained rate of shear strength increase with increasing shear reinforcement ratio ρ_s is somewhat lower than in empirical formulas, but matches well the prediction by the exact truss analogy for which the shear carried by stirrups is equal to: $v_s = \rho_s f_{sy} ctg\alpha$. The angle of major inclined crack α increases (and $ctg\alpha$ decreases) with increasing reinforcement ratios. However, in most code provisions and empirical formulas it is assumed that $v_s = \rho_s f_{sy} K$ in which the constant multiplyer K does not depend on ρ_s. The consequence is a steeper increase of the ultimate shear stress then in the case with $K = ctg\alpha$.

		no stirrups	$\phi 6mm$	$\phi 8mm$	$\phi 10mm$	$2\phi 8mm$
A_s	$[mm^2]$	-	56.5	100.5	157.1	201.1
Load	a	259	291	320	345	384
Case	b	282	308	330	381	428
	c	306	338	375	427	485

Table 1. Ultimate Force P_u (Reaction at the Support) in $[kN]$

The values of ultimate shear force in Table 1, and ultimate shear stresses in Fig. 5 reveal higher shear strengths for load cases b and c than for load case a. The reason is a shift from a concentrated load (load case a) towards a more uniformly distributed load (load cases b, c). According to test results, under otherwise constant conditions, the shear strength of a beam with distributed loads is higher than for concentrated loads. This change of loading arrangement represents a change of the shear span ratio and precludes the direct comparison between load case a and load cases b, c.

To study the influence of anchor loads on the shear strength of beams, load cases b and c which have the same shear span ratio are compared. The placement of anchoring elements in the bottom zone (load case b) results in a lower shear strength than for the beam where all loads are applied on the top surface (load case c). The measure of decrease is obtained from a comparison of the ultimate loads by:

$$\Delta P = \frac{P^c - P^b}{P^c} \tag{8}$$

in which superscripts denote load cases. Obtained values are presented in Fig. 7. The results show that the difference of shear strength is within the range of 8 - 11%. The higher shear strength for load case c is explaned in Fig. 8, where from the free body diagram follows that a part of the top load is directly transferred to the support. In contrast to that, the bottom load must be transferred to the top zone by stirrups before being transferred to the support by diagonal struts. Details concerning the decrease of shear strength are discussed in [4]. In the present analysis, the decrease of shear strength for the beam without shear reinforcement is about 8%. This is somewhat higher than found in a similar analysis performed by Cervenka et al. [2] for beams without shear reinforcement where 100% of the load is applied in the bottom zone and a decrease of 8-10% is obtained.

5. CONCLUSIONS

The performed analysis gives an insight into the behavior of reinforced concrete beams which are loaded by a concentrated load on the top surface and by equally distributed loads over the top or bottom zones. The analysis shows that loads introduced into the bottom zone by headed anchors might negatively influence the shear carrying capacity. The effects of different load arrangements are outlined.

References

[1] Bazant, Z. P. and Oh, B. H., "Crack Band Width Theory for Fracture of Concrete", *Materiaux et Constructions,* Vol. 16, 1983, pp.155-177.

[2] Cervenka, V., Pukl, R. and Eligehausen, R., "Computer Simulation of Anchoring Technique in Reinforced Concrete Beams". *Proceedings,* Second International Conference Computer Aided Analysis and Design of Concrete Structures, Zell am See, Austria, April 1990, Pineridge Press.

[3] Eligehausen, R., Fuchs, W., Lotze. D. and Reuter, M., "Befestigungen in der Betonzugzone", *Beton und Stahlbetonbau,* Vol. 84, 1989, pp.27-32. and 71-74.

[4] Kazic, M. and Eligehausen, R., "Numerical Simulation of Shear Problems of Reinforced Concrete Beams", Report in preparation, Institut für Werkstoffe im Bauwesen, Universität Stuttgart, 1990.

[5] Kolmar, W., "Beschreibung der Kraftübertragung über Risse in Nichtlinearen Finite Element Berechnungen von Stahlbetontragwerken", Dissertation, T.H. Darmstadt, 1985, 94 p.

[6] Kordina, K. and Blume, F., "Empirische Zusammenhänge zur Ermittlung der Schubtragfähigkeit stabförmiger Stahlbetonelemente", Deutsche Ausschuss für Stahlbeton, Heft 364, Berlin 1985.

[7] Mallèe, R., "Zum Schubtragverhalten stabförmiger Stahlbetonelemente", Deutsche Ausschuss für Stahlbeton, Heft 323, Berlin 1981.

[8] Specht, M., "Zur Querkraft Tragfähigkeit im Stahlbetonbau", *Beton und Stahlbetonbau,* Vol. 84, 1989, pp.193-198.

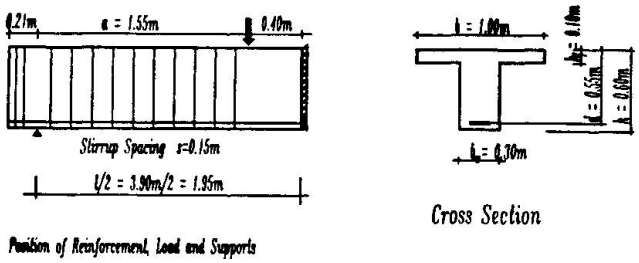

Fig.1 Dimensions of the Analysed Beam

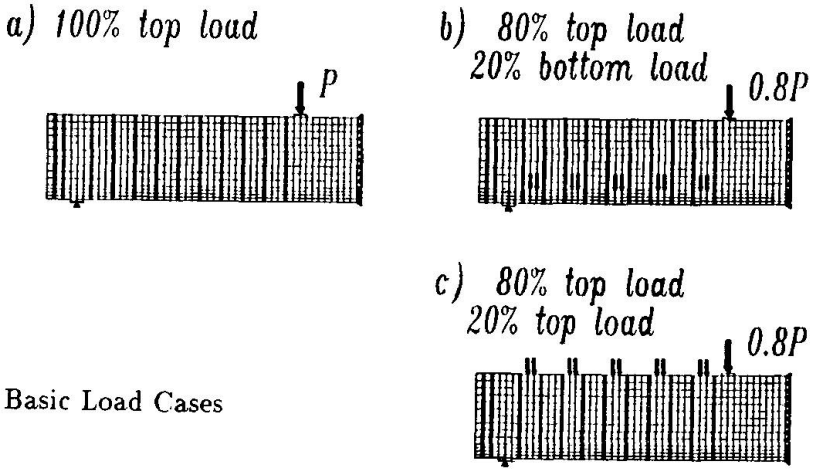

Fig.2 Basic Load Cases

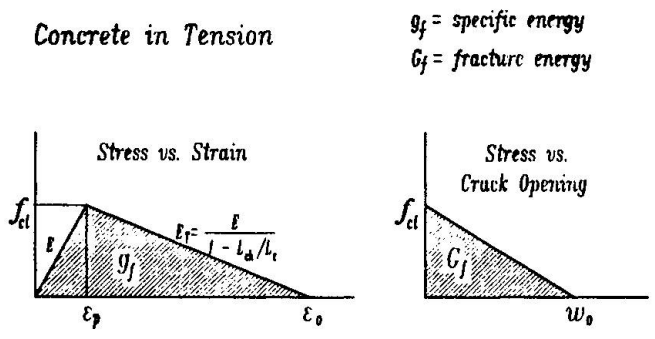

Fig.3 Concrete in Tension

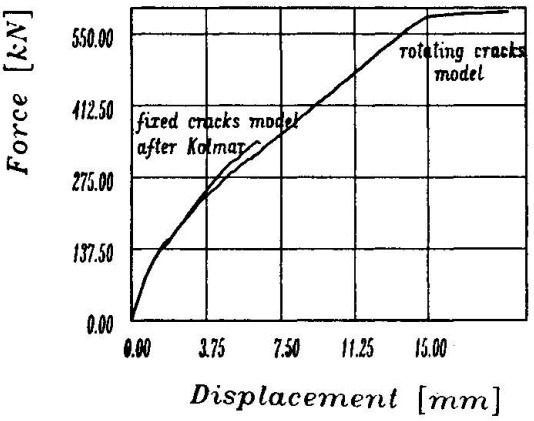

Fig.4 Influence of Crack Model

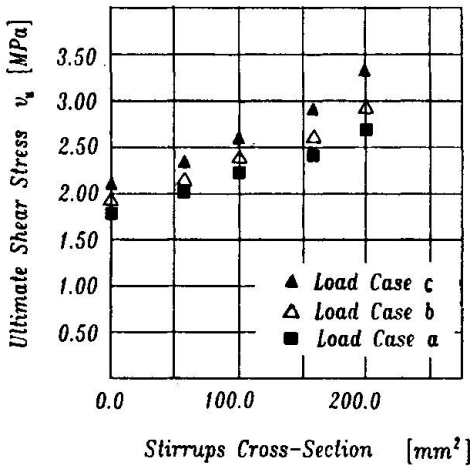

Fig.5 Ultimate Shear Stresses

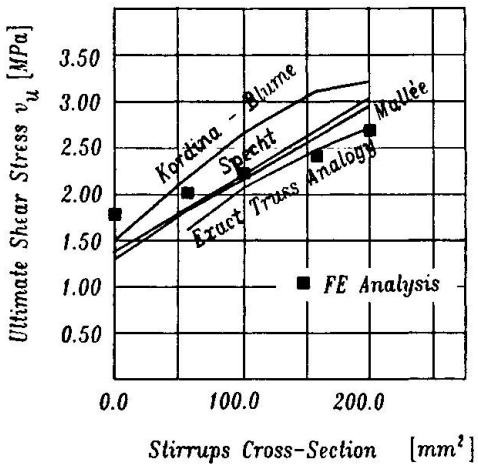

Fig.6 Results vs. Empirical Formulas

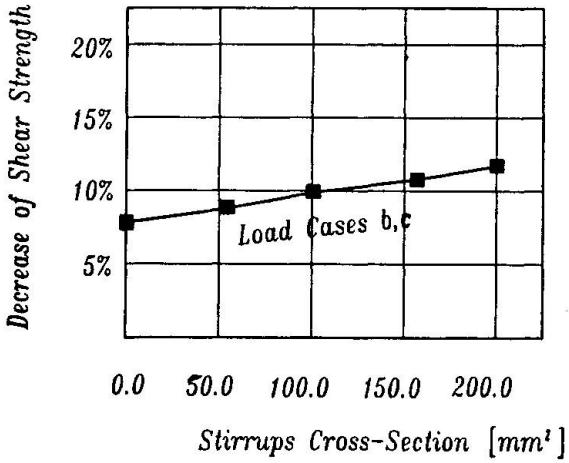

Fig.7 Decrease of Shear Strength

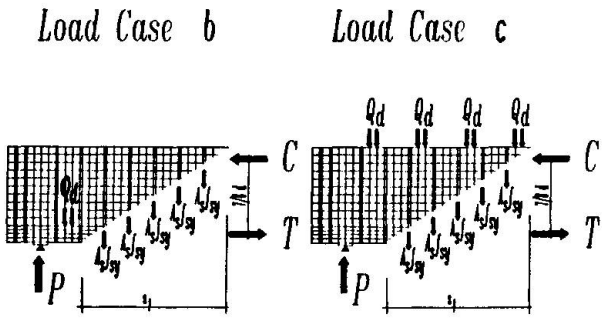

Fig.8 Free Body Diagrams

Load Carrying Mechanism of Anchor Bolt

Résistance d'un boulon d'ancrage chargé

Tragfähigkeit von Ankerbolzen

Kyuichi MARUYAMA
Assoc. Prof.
Nagaoka Univ. of Technology
Nagaoka, Japan

Kyuichi Maruyama, born 1948, received Ph.D. from the University of Texas at Austin in 1979. His research interests include durability of reinforced concrete structures.

Keiji SHIMIZU
Prof.
Nagaoka Univ. of Technology
Nagaoka, Japan

Keiji Shimizu, born 1928, received Doctor of Agriculture from the Univ. of Tokyo in 1971. He has extensive experience in railroad engineering.

Mitsuhiro MOMOSE
Civil Engineer
Nagano Pref. Office
Nagano, Japan

Mitsuhiro Momose, born 1966, received Master of Engineering from Nagaoka University of Technology in 1990.

SUMMARY
It is discussed in this paper how an anchor bolt, embedded in concrete, carries the applied load under static and fatigue loadings. An experimental test was conducted using anchor bolts of relatively small size in diameter and length. Examining the failure mode of concrete in detail, a mechanical model is developed in terms of an angle of crack propagation, stress distribution and the tensile strength of concrete.

RÉSUMÉ
Ce rapport décrit la façon dont un boulon d'ancrage dans le béton supporte l'application d'une charge statique et endure la fatigue. L'expérience a été menée sur des boulons d'ancrage relativement de petite taille (longueur et diamètre). Après observation du mode de rupture du béton environnant, un modèle mécanique est développé en fonction de l'angle de propagation de la fissure, de la distribution des contraintes et de la résistance du béton à la traction.

ZUSAMMENFASSUNG
In diesem Aufsatz wird erörtert, wie ein im Beton eingebetteter Ankerbolzen die Last unter statischen und ermüdenden Belastungen trägt. Der Versuch wurde mit in Durchmesser und Länge relativ kleinen Ankerbolzen durchgeführt. Nach sorgfältiger Prüfung des Betonbruchs wurde ein mechanisches Modell unter Berücksichtigung des Winkels des Rissfortschritts, der Verteilung der Spannung und der Zugfestigkeit des Betons entwickelt.

1. INTRODUCTION

The authors have reported the characteristics of the newly developed fixings (undercut type fixings) in terms of the static and fatigue strength, the applicability near the edge or the corner of concrete structures [1]. In the paper the empirical formulas were proposed for estimating the static and fatigue strength of such type fixings based on the experimental results. However, the formulas were limited to the fixings having 40 mm embedment length because of the limited range of test data. It was necessary to extend the study on the load carrying mechanism of the fixings from the low load level up to the failure stage with variations of embedment length and dimension of bolt.

In order to develop a general model of load carrying mechanism of the fixings, the static pull-out test was first conducted varying both the embedment length of bolt and the location of bolt from the edge of concrete block specimen. Referring to the study on application of acoustic emission to the pull-out test of anchor bolt [2], the discussion was extended to how the concrete carried the applied load, and what was the rational expression for the load carrying capacity of the undercut type fixings. The study should be applicable to the load carrying mechanism of ordinary anchor bolt because the load transfer point from the bolt to the surrounding concrete of this fixings is similar to that of ordinary anchor bolt.

2. EXPERIMENT

2.1 Bolts

The main parameters in the experiment were the size (diameter) and the embedment length of bolt. The shape of bolt is shown in Fig.1 and the dimension is summarized in Table 1. The tensile strength of bolt was 800 MPa. In order to assure the anchorage of bolt, the torque listed in Table 1 was applied to a bolt in advance of the pull-out test.

Concrete Block (cm)	Size of bolt (mm) d le	Φ	D	Torque (KN·cm)
50x50x20	14x40	M10	18	2.35
60x60x30	14x60	M10	18	3.53
	18x80	M12	24	6.76
120x60x30	22x100	M16	28	11.8

Table 1 Dimension of bolt

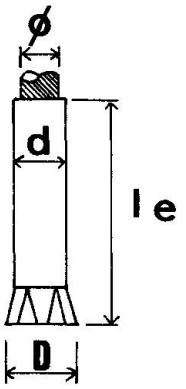

Fig.1 Shape of bolt

2.2 Test Setup

Fig.2 shows the test setup. The load was applied to a bolt by a center hole type oil jack, and was measured by a load cell of 50 KN or 200 KN capacity. The displacement was measured by LVDT-'s. In order to avoid the confinement effect due to the reaction supports, the supports were placed 3 times of embedment length (3·le) away from the bolt.

All the data were recorded and stored in a microcomputer through a dynamic strain meter and an A/D converter. The similar system was used for the fatigue test. The strength of concrete block specimen was evaluated by the compressive strength test using a cylindrical specimen of Φ10x20 cm.

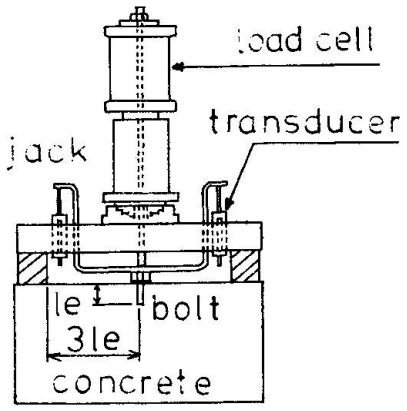

Fig.2 Test setup

3. TEST RESULTS AND DISCUSSION

After the pull-out test, the failure mode of the specimen was examined concerning with the shape of ruptured cone of concrete. A typical projection of cone is shown in Fig.3. The failure surface can be simplified as a tri-linear line as shown in Fig.4. Near the bottom end of bolt the concrete was splitted, and the crack developed at an angle of Φ from the horizontal. At a certain point the angle of crack propagation turned to θ. Finally, the ruptured cone was pulled out with the skirt of shallow angle near the surface of concrete.

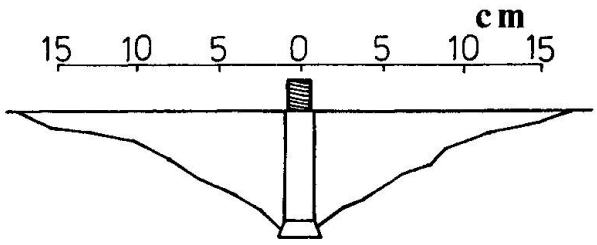

Fig.3 Ruptured cone

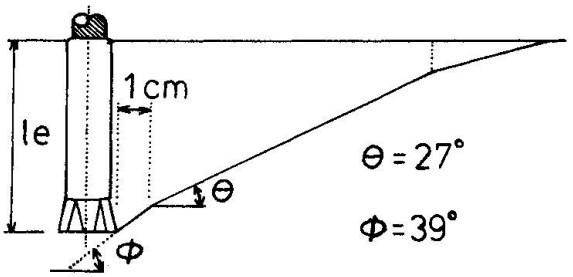

Fig.4 Simplified cone

Since the measurement of cone depth was done in the four directions, Table 2 shows four values of Φ and θ. The shallow angle of the skirt of cone was not shown because it was less important in the load carrying mechanism as will be discussed in the next section. The first angle (Φ) ranged from 26 to 50 degree, and the second one (θ) from 20 to 40 degree. There observed little influence of the diameter and the embedment length of bolt, and of the concrete strength on the angles. The mean values were 39 and 27 degree for Φ and θ, respectively. Some data of Φ are not shown because too much rupture of concrete made the measurement of angle impossible. The location of turning point of the crack angle from Φ to θ was observed scarcely influenced by the embedment length of bolt and the concrete strength. In the test it was about 1 cm away from the center of bolt (Fig.4). The examination was extended to the mortar block. The results were similar to those of concrete block, showing Φ=36 and θ=24 degree.

Bolt d le Φ	f'_c MPa	f_t MPa	Φ (degree)	θ (degree)	P_{max} KN
14x40 M10	19.2	1.75	41 34 48 -- 36 43 27 --	28 20 48 25 24 30 27 27	20.7 20.8
14x60 M10	38.7	2.84	-- -- -- -- 47 42 46 -- 37 45 48 35	26 20 27 45 29 27 27 25 15 18 21 25	44.1 55.0 38.4
18x80 M12	31.4 38.7 37.3	2.24 2.84 2.52	45 38 -- -- 29 32 53 45 49 41 -- --	30 30 25 30 24 35 21 29 21 26 23 22	61.9 65.7 55.0
22x100 M16	37.3	2.52	37 26 41 30 35 30 36 -- 38 54 -- --	37 28 24 38 30 30 31 16 34 32 -- --	90.6 86.2 109
14x40 M10	37.4*	2.39	42 33 51 20	27 24 26 20	22.3
Mean Value Standard Deviation Coeff. of Variation			39.2 8.2 20.8 %	27.1 6.5 24.0 %	

* : Block was made of mortar.

Table 2 Test results

4. MODELLING OF LOAD CARRYING MECHANISM

Before constructing a mechanical model, the pertinent researches were surveyed. Rokugo et al [2] reported that up to the maximum load level the acoustic emission in the pull-out test generated within the circle area having the radius of 1.6 times of embedment length (1.6·le; Figs.5,6). On the other hand, the finite element analyses done by Kamimura [3] and Kosaka [4] showed that the principal tensile stress became to zero at the location of (1.7-1.8)·le away from the center of bolt. The similar results were obtained by the other series of test which examined how the pull-out resistance of anchor bolt was influenced by varying the bolt location from the edge of concrete block.

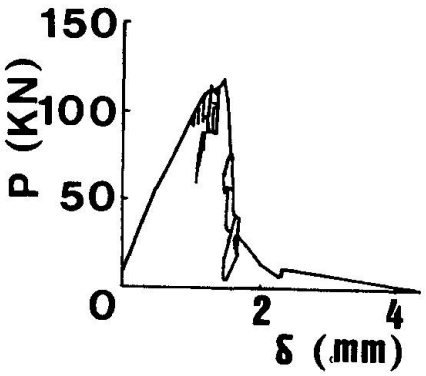

Fig.5 Load-displacement [2]

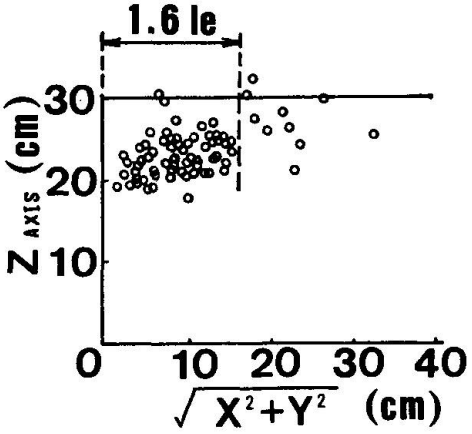

Fig.6 Acoustic emission [2]

Taking these results into account, the load carrying mechanism of anchor bolt was modelled on the following assumptions (See Fig.7).

(1) Crack initiates and propagates along the assumed cone line as shown in Fig.4.
(2) At the tip of crack (distance of x from the bolt center in Fig.7), the applied load is resisted by both the splitting strength of uncracked portion of concrete (outside the tip of crack) and the frictional resistance of cracked portion (inside the tip of crack). The distribution of resistant stress is assumed to be an isosceles triangle.
(3) Crack begins to propagate when the stress at the tip of crack exceeds the modulus of rupture of concrete (f_{tx}).
(4) The modulus of rupture of concrete depends upon the confinement condition of concrete. As shown in Fig.7 the modulus of rupture near the bottom end of bolt is assumed to be 1.2 times of (f_t) which is given by the standard test [5]. The confinement effect decreases and fades out at the location of 1.7·le away from the center of bolt.
(5) The fraction of resisting stress is neglected near the bottom of bolt where the concrete was splitted, and is neglected outside the projected circle range of 1.7·le radius.

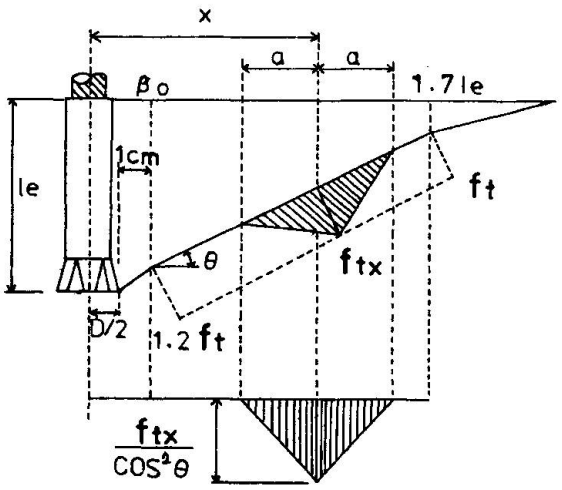

Fig.7 Proposed load carrying mechanism

The load corresponding to a given resistant stress distribution is, then, calculated as follows:

$$P = \frac{\pi \cdot f_{tx}}{\cos^2\theta} \cdot (2 \cdot a \cdot X) - A \qquad (1)$$

where, A :modification factor due to imperfect shape of stress distribution.

The ultimate capacity of fixings is, then, calculated so as to find the maximum value of P in Eq.(1) in the supposed failure surface. In addition, the resistant stress conditions could be correlated to the load-displacement curve in Fig.8. For example, at stage 1 , the deformation is mainly attributed to the elastic deflection of bolt. During stages 2 through 3, crack propagates at an angle of θ and the cracked portion of concrete is lifted up. The displacement may be due to the flexural deflection of cracked portion.

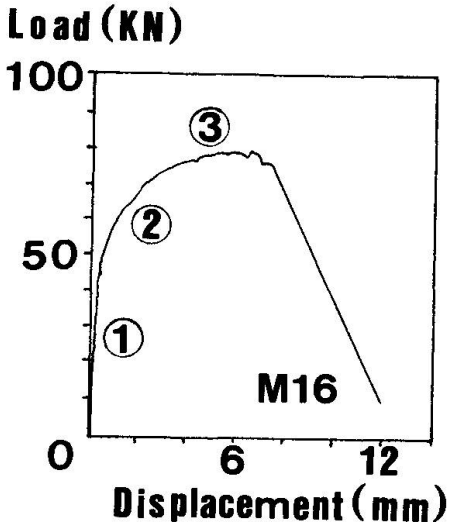

Fig.8 Load-displacement

5. COMPARISON OF CALCULATION WITH TEST

5.1 In general

For calculation by the model, it is necessary to determine the angle of θ and the base length (a) of the shape of stress distribution in advance. In this study the angle of θ was fixed as 27 degree which was the mean value of the experimental results. On the contrary, there was not any rational method to determine the length (a) at this moment. Then, the length (a) was chosen as 2.7 cm which was the best fit value to the test results after several trial and error calculations. Fig.9 shows the comparison of calculated results with test results having the factor of correlation of 97.5 %.

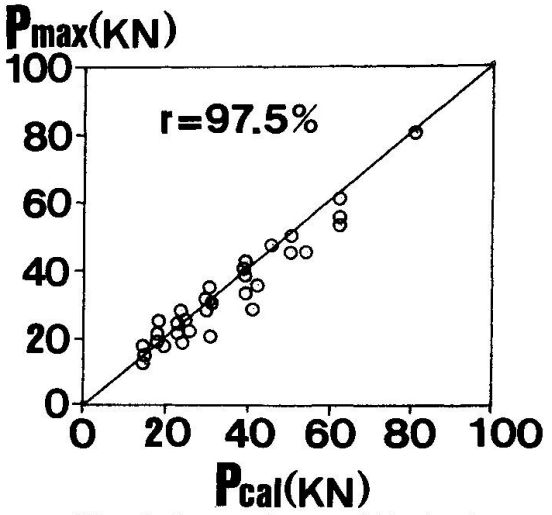

Fig.9 Comparison with test

5.2 Near Edge

The model with the same values of θ and (a) was applied to the case in which the bolts were mounted near the edge of concrete block. The resistant stress outside the edge was naturally neglected as shown in Fig.10. The comparison is shown in Fig.11. The factor of correlation was 91.9 % which was slightly less than that of general cases. This may be attributed to (1) the less confinement effect near the edge of concrete block, and (2) the difference of the failure pattern from the assumed one. However, the value of 91.9 % might not be so bad in prediction.

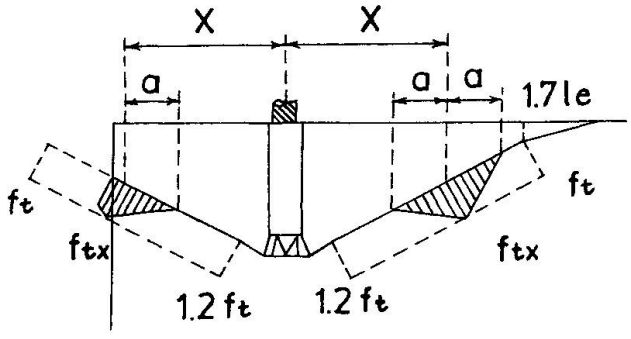

Fig.10 Stress distribution near edge

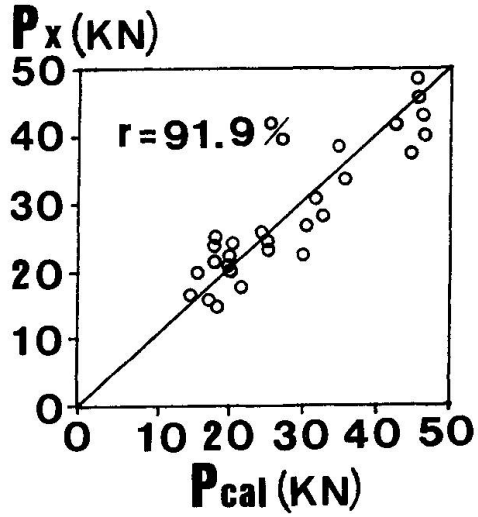

Fig.11 Comparison with test

6. FATIGUE CAPACITY OF FIXINGS

Varying the applied cyclic load level, the fatigue life of fixings was examined. The test results are plotted in Fig.12, where the solid circles represent the cases of bolt fracture and the open circles are those of concrete rupture in a conical shape. The solid line is drawn from the equation for the fatigue life of bolt (Eq.2), and the broken lines are from the equation for concrete (Eq.3). Both equations are proposed by the Japan Society of Civil Engineers [6].

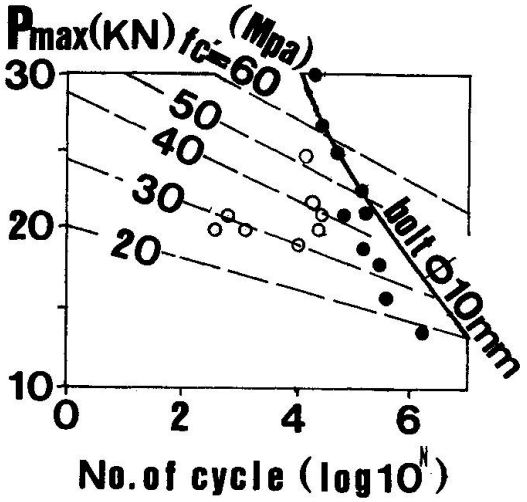

Fig.12 Fatigue Capacity

$$f_{srd} = 1900 \cdot (10^{\alpha}/N^{k}) \cdot (1-\sigma_{sp}/f_{ud}) \qquad (2)$$

where, $\alpha = 0.82-0.003\Phi$, $k = 0.12$,
Φ = diameter of bolt (mm).

$$\log N = 17 \cdot \{1-(\sigma_{max}-\sigma_{min})/(f_u-\sigma_{min})\} \qquad (3)$$

where, σ_{max} = maximum stress in concrete due to the model, σ_{min} = minimum stress and f_u = static strength.

7. CONCLUSIONS

The followings were concluded from this study.

(1) The resistance of concrete against the pull-out force of bolt may be attributed to the area within the projected circle with a radius of 1.7 times of the embedment length of bolt.
(2) The pull-out resistant capacity of the fixings can be predicted by the proposed model. The model is also applicable to the fixings used near the edge of concrete structures.

REFERENCE

[1] MARUYAMA, K., MOMOSE, M. and SHIMIZU, K., Mechanical Behavior of Undercut Type Fixings. Transactions of the JCI, Vol.11, 1989, pp.531-538.
[2] ROKUGO, K. and et al,Pull-out test of anchor bolts and examination of failure processing by means of acoustic emission. Proceedings of the JSCE 43rd annual meeting, Part 5, 1988, pp.418-419. (in Japanese)
[3] KAMIMURA, K. and et al, Influence of Concrete Properties upon Pull-out Strength of Mechanical Anchor Embedded in Concrete Members. Proceedings of JCI, Vol.8, 1986, pp.405-408. (in Japanese)
[4] KOSAKA, Y. and et al, Effects of Various Factors on Pull-out Strength of Hole-in Anchors Embedded into Hardened Concrete. Proceedings of CAJ 36th General Meeting, 1982, pp.195-198. (in Japanese)
[5] OHTANI, Y. and et al, Failure mechanism of stud anchor in tension. Proceedings of the JSCE 43rd annual meeting, Part 1, 1988, pp.372-373. (in Japanese)
[6] JAPAN SOCIETY OF CIVIL ENGINEERS, Standard Specification for Design and Construction of Concrete Structures - 1986, Part I (Design). 1986, p.244.

Pull-Out Test of Anchor Bolts Embedded in Concrete

Test d'arrachement du boulon d'ancrage dans le béton

Ausziehversuche von Ankerbolzen im Beton

Gianfranco VALENTE
Assoc. Professor
Univ. de l'Aquila
L'Aquila, Italy

Gianfranco Valente, born 1943, received his civil engineering degree at the University of Rome in 1967 Assistant Research in Rome until 1986.

SUMMARY

An incremental-iterative procedure for the nonlinear finite element analysis of reinforced concrete structures is adopted here. Solid concrete is modelled as a hypoelastic material, whilst cracked concrete (including fracture and aggregate interlock) is modelled with crack bands, according to the smeared crack approach. The proposed approach is applied to the analysis proposed by RILEM TC-90 FMA regarding pull-out tests of anchor bolts in concrete. Only the plane stress condition is considered in this paper.

RÉSUMÉ

On adopte ici une procédure itérative et incrémentale dans le cas de l'analyse non-linéaire de structures en béton armé. Le béton sain est modélisé par un matériau hypoélastique, tandis que le béton fissuré (includant fractures et déchaussements des agrégats) est modélisé par des «bandes de fissuration», ceci en accord avec l'aspect-même des fissures apparues. Cette approche est appliquée à l'analyse proposée par RILEM TC-90 FMA, concernant le test d'arrachement d'un boulon ancré dans le béton. On ne considére dans cet article que l'état de contrainte bidimensionnel.

ZUSAMMENFASSUNG

Ein inkrementelles Iterationsverfahren wurde für eine nichtlineare Finite-Element-Analysis von Stahlbetonbauten verwendet. Beton wird als ein hypoelastischer Werkstoff dargestellt, hingegen wird gerissener Beton (Bruchmechanik und Kornverzahnung) mit Rissbändern, nach dem «smeared crack»-Verfahren dargestellt. Das vorgeschlagene Verfahren wird für die vom RILEM TC-90 FMA vorgeschlagenen Analysis, Ausziehungsversuchen von Betonankerschrauben angewendet. Es wird nur ein ebener Spannungszustand berücksichtigt.

1. INTRODUCTION

Tensile failure in concrete occurs when the tensile stress in one principal direction exceeds the tensile strength. In this case the usual assumption that a plane of failure develops at right angle to the previous principal direction is introduced. Tensile cracking is identified using failure surfaces fixed at the onset of the cracking. The smeared crack concept for fracture and aggregate interlock is adopted . As regards fracture, it is easier to use compliance rather than stiffness matrices, and it suffices to adjust some terms of the compliance matrix. Instead, for aggregate interlock it is easier to use a stiffness matrix approach and it suffices to adjust four terms of this matrix, which is nonsymmetric and does not yield coincident principal axes for stress and strain increments because shear and normal components are coupled. As a general rule, in concrete models, after tensile cracking, the normal stress is released completely (ADINA [1]) and some coefficients of the concrete stiffness matrix are reduced with two constant factors (ADINA, DIANA [1], [5]). Isoparametric elements with a maximum of eight nodes and four integration Gauss points in each direction are used. For concrete, we must take into account three different angles at each integration point for: failure plane, principal strains, principal stresses [9]. The tangent stiffness matrix is referred to:

- principal stress directions, before tensile failure;
- failure coordinate system (axes parallel and transverse to the crack planes) after tensile failure.

The tensile failure envelope given in Fig.1 is employed. It may be observed that compressive stress change this tensile strength. The nominal stress at failure decreases as the size increases. This is caused by the fact that in the presence of the softening the failure cannot be simultaneous but must occur through propagation of a failure across the structure. In a larger structure, this nonsimultaneous nature of failure is more pronounced. In pullout failure, the existence of the size effect must clearly be expected, due to the brittle nature of these failures.

2. RELATIONSHIP BETWEEN THE STRESSES AND THE CRACK OPENING IN FRACTURE

The simplifing assumption that the descending branch is a straight line is adopted here. The analytical curve is shown in Fig.2a). The material behaves in the nonlinear way shown in Fig 2b), where:

- E_0 is the Young's modulus of concrete;
- the quantity of energy absorbed per unit crack area when the crack widens from zero up to or beyond δ_0 is represented by the area lying between the curve and the ϵ axis:

$$w \int \sigma(\epsilon) d\epsilon = G_F \tag{1}$$

Then, from Fig.2b:

$$\epsilon_1 = \sigma/E_0 + \delta/w \tag{2}$$

$$\epsilon_p = \sigma_t/E_0 \tag{3}$$

$$1/C_f + 1/E_0 = 1/E_t \tag{4}$$

$$G_F = (2.72 + 3.10\ \sigma_t)\ \sigma_t^2\ d_a/E_0 \qquad \text{(from [2])} \tag{5}$$

3. AGGREGATE INTERLOCK CONSTITUTIVE LAWS

The "Rough Crack Model" initially proposed by Bažant and Gambarova [3], and later improved ([4], [8], [9], [10]), is here adopted:

$$\sigma_{nn} = a_{12} r \sqrt{\delta_n}\ \sigma_{nt}/h \tag{6}$$

$$\sigma_{nt} = \tau_0 \left(1 - \sqrt{2\,\delta_n/d_a}\right) r\,(f/g) \quad (7)$$

where:

$$f = a_3 + a_4 |r^3| \quad (8)$$

$$g = 1 + a_4 r^4 \quad (9)$$

$$h = (1+r^2)^{1/4} \quad (10)$$

$r = \delta_t/\delta_n$, $a_{12}=0.62$, $a_3 = 2.45/\tau_0$, $a_4 = 2.44(1-4/\tau_0)$, $\tau_0 = 0.25\,\tilde{\sigma}_c$,

d_a = maximum aggregate size (3.5mm in the present paper), from (5).

FIG.1-Plane Tensile failure Envelope of Model.(——)Code,(---)Kupfer et al.

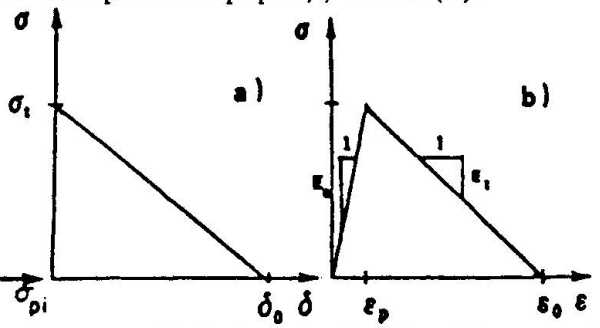

FIG.2-Stress-Strain Diagrams for Fracture.

4. ANALYSIS OF ANCHOR BOLTS IN CONCRETE

The material properties are as follows:

E_0 = 30000 N/mm^2 initial tangent modulus;

ν = 0.2 Poisson's ratio;

$\tilde{\sigma}_t$ = 3.0 N/mm^2 uniaxial tensile strength;

$\tilde{\sigma}_c$ = -40.0 N/mm^2 uniaxial compressive strength;

ϵ_c = -.0022 uniaxial crushing strain;

ϵ_u = -.0031 uniaxial ultimate strain;

β = 0.6 stress ratio for failure surface input;

γ = 1.0 strain scaling factor for multiaxiality;

k = 0.6 control for iso/orthotropic material law;

α = .01 control for loading/unloading chriterion;

$l_{ch} = E_0 G_F/\sigma_t$ = 333.3mm characteristic length.

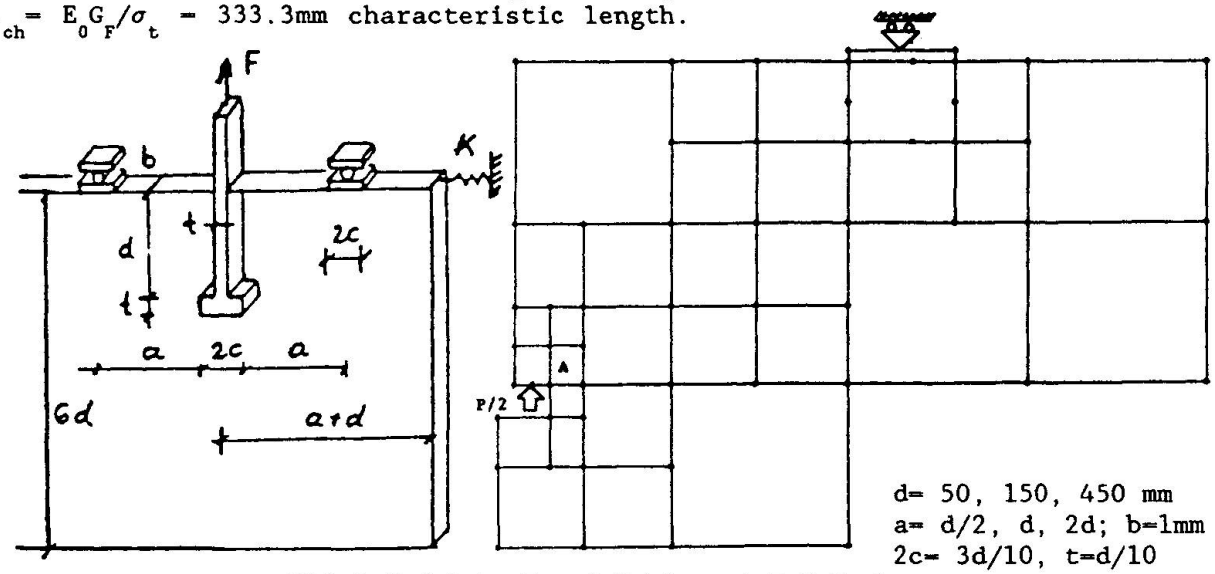

FIG.3-Model by Round Robin and F.E.Mesh.

The finite element mesh is shown in Fig.3. The load is applied at point A. For the unit width b=1.mm, the load-displacement curves of the full slab are shown in Fig.4 and have the maximum values P_u, δ_u as in Table I. Within the deadline of the Round Robin [11], the Author performed a case alone for d=150mm, a=d, K=0. But the final results gathered in [11] compelled himself to extend the analysis to all the six cases for a=d in order to complete the comparisons, expecially with Cervenka and Ozbolt.

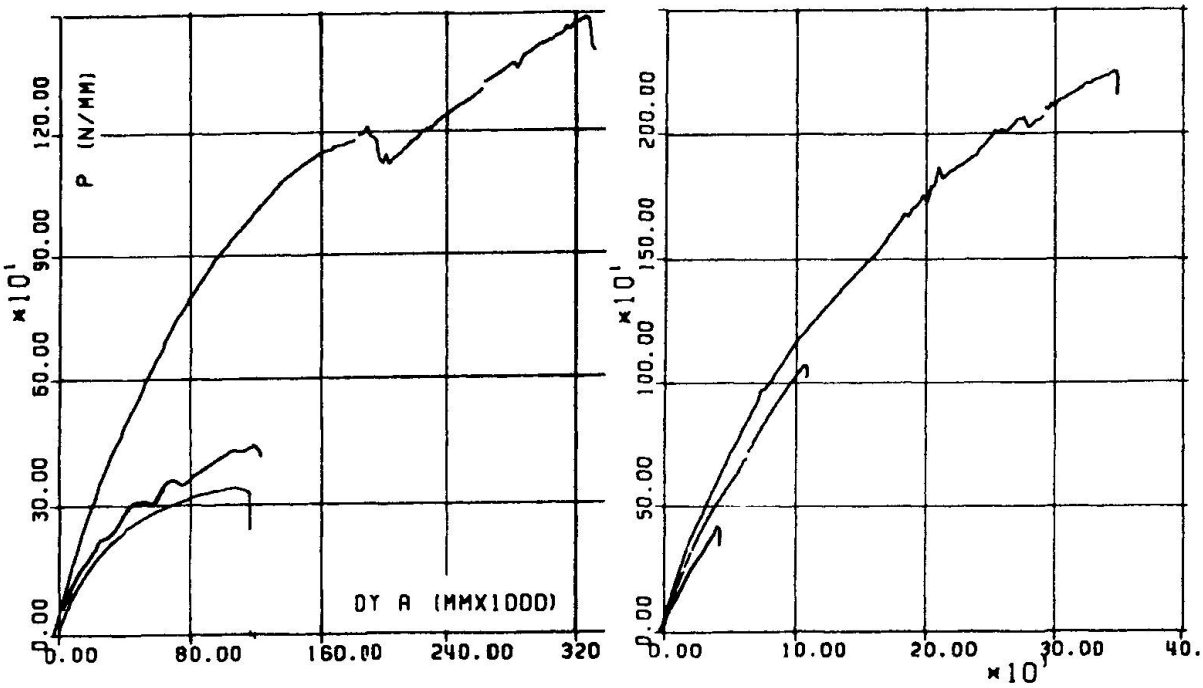

K=0 FIG.4- Load-Displacement Curves. K=∞

TABLE I-Maximum Loads and Displacements P_u/δ_u [N/μ], ([11]).

K=	0			∞		
d [mm]	50	150	450	50	150	450
Ozbolt	175/35	427/90	934/185	328/60	804/200	1790/400
Author	338/107	440/116	1469/327	414/40	1063/110	2232/346
Cervenka(f)	318/100	472/115	1090/340	690/120	1307/310	2549/600

Some of the features of the solution process are:
- both material and geometrical nonlinearities are considered;
- only prescribed displacemets are used;
- the load steps are performed in such a way that the peaks of the stress-strain curves for tensile stresses are matched within +2% (Fig.2b);
- the strain-softening range runs for at least 2 steps;
- the stiffness matrix is updated at each step;
- the equilibrium iterations are performed during each step, with the following tolerance on convergence:

  ($0.5\%P_u$) maximum allowed unbalanced load norm,

  1% for the norm of unbalanced incremental energy.

5. BAŽANT-SIZE-EFFECT-LAW

In concrete structures, the size effect [6] is intermediate between the linear elastic fracture mechanics, for which is much too strong, and the plastic

limit analysis, for which it is absent. These laws are represented in Fig.5. B is the negative slope of the tangent to the curve in Figs.5c,d. This slope approaches that of linear fracture mechanics for increasing d. In terms of sensitivity, it seems that in these cases the value of B is close to 0.5. One consequence of this is also that the formal stress associated with pull out of a bolt is very size-dependent.

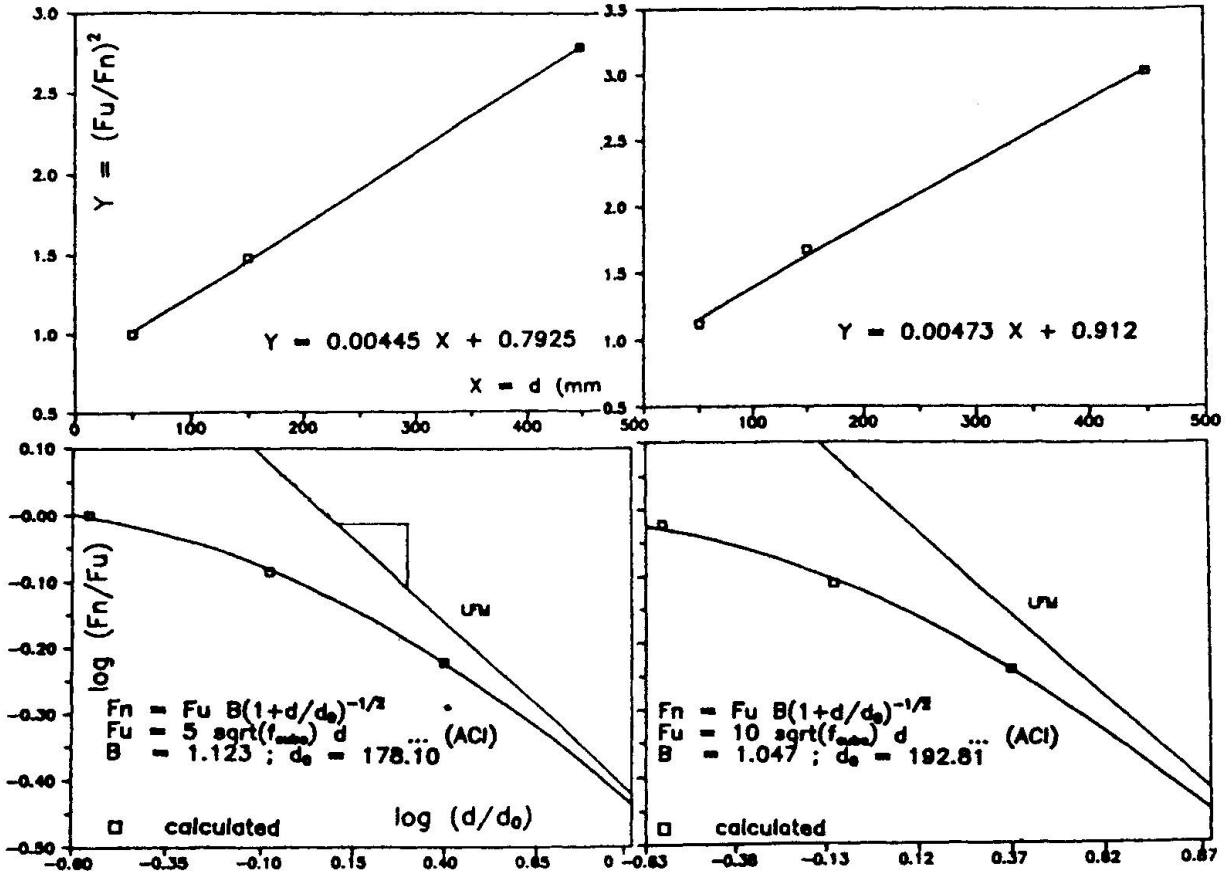

K=0 FIG.5-Bažant-Size-Effect-Laws [6](Figs.by Ozbolt[11]). K=∞

6. CONCLUDING REMARKS

Within this research project, a pre-existing F.E.program for the nonlinear analysis of R.C.elements has been implemented with suitable models for concrete fracture and aggregate interlock.

In principle, the model for tensile fracture can be applied in analysing all the cases where we need to rely on the tensile strength of concrete . We are still far from a sufficient understanding of all types of tensile-induced structural failures. Some of them are very complicated to analyse. A major research effort is needed within this area in order to achieve better guidelines for design rules. Such a research effort may be expected to lead a more even safety factor and large savings. The anchorage of bolts is a case which can be teoretically analysed , although it is rather complicated, because not only tension, but also shear stresses act in the fracture zone, and several fracture zones may have to be taken into account. In order to compare different analytical methods,an invitation was given to a round robin of this common structural detail. Here, comparison with more test results was done. The Code proposed by Cervenka [11] (with fixed cracks) seems very close to that one of the Author. Instead, Ozbolt [11] use a refined nonlocal microplane model. Some of the features of this comparison are:

- the shapes of the load-displacement curve are very similar;

- there is a certain scatter for the values P_u/δ_u that can be ascribed to different meshes, different constraint, different shear reduction factors.

For the Bažant-Size-Effect-Law, it may be conclude that:

1. The present analysis results confirm that a size effect is present, i.e. the nominal shear bond stress at failure decreases as the specimen increases.
2. It appears rhat the results are consistent with Bazant's approximate size effect law for failures due to distributed cracking, as should be theoretically expected according to the known failure mechanism.
3. The analyses indicate that larger specimens tend to fail in a more brittle mode, while smaller specimens tend to fail in a less brittle mode or more plastic shear-pullout mode. This transition in the type of failure as a function of specimen size is in agreement with the physical implications of the size effect law and supports its applicability.

ACKNOWLEDGEMENTS

This research is a part of a comprehensive project on the mechanical behavior of concrete elements, which was supported from the Italian Ministry of Education (M.U.R.S.T. 40% 1989).

REFERENCES

1. K.J. Bathe and S. Ramaswamy, On Three Dimensional Nonlinear Analysis of Concrete Structures, Nuclear Engineering and Design, Vol.52, 1979, pp.385-409.
2. Z.P. Bažant and B.H. Oh, Crack Theory for Fracture of Concrete,Vol.16,n.93, Materiaux et Constructions.
3. Z.P. Bažant and P.G. Gambarova, Rough Cracks in Reinforced Concrete, Jrn.of the Structural Division, ASCE, Vol.106, No.4, April 1980, pp.819-842.
4. S. Dei Poli, P.G. Gambarova and C. Karacoç Aggregate Interlock Role in R/C Thin-Webbed Beams in Shear, Journal of Structural Engineering, ASCE,Vol.113 No.1, January 1987, pp.1-19.
5. J.G.M.Van Mier, "Examples of non-linear analysis of reinforced concrete structures with DIANA", Heron, Vol.32, 1987, no.3.
6. Z.P.Bažant, S.Şener,"Size Effect in Pull Out Test", ACI Materials Journal, Sep-Oct 1988.
7. L.Elfgren,"Fracture Mechanics of Concrete Structures.From Theory to Applications", a RILEM Report prepared by TC 90-FMA, edited by Elfgren Chapman & Hall, 1989.
8. P.G.Gambarova, G.Valente,"Fracture and Aggregate Interlock Mechanism in R/C SMiRT 10, Div.Q, August 1989, Ca, USA.
9. P.G.Gambarova. G.Valente,"Smeared Crack Analysis for Fracture and Aggregate Interlock in Concrete", Engineering Fracture Mechanics, Vol.35, No.4/5,pp. 651-663, 1990.
10. M.Di Prisco, P.G.Gambarova, G.Valente, "Evolutive vs Limit Analysis in Modelling R/C Thin Webbed Beams failing in Shear", 2nd Int.Conf.on Computer Aided Analysis and Design of Concrete Structures, Austria, April 1990.
11. L.Elfgren, "Round Robin Analysis of Anchor Bolts", RILEM TC-90 FMA, Preliminary Report, September 1990.

Stresses and Strains in a Model Ring under Internal Radial Pressure

Contraintes et déformations dans un anneau soumis à une pression radiale intérieure

Spannungen und Verformungen im Betonring-Modell unter Radialdruck

Juraj BILČÍK
Civil Eng.
Techn. Univ.
Bratislava, Czechoslovakia

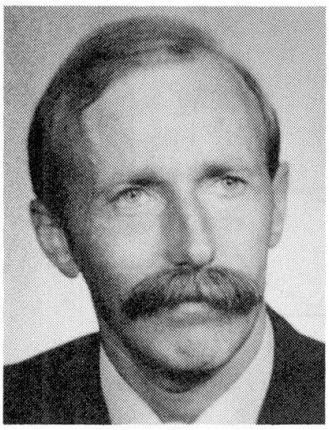

Juraj Bilčík, born 1947, obtained his civil engineering degree at the Slovak Technical University Bratislava, where, he is currently working as a reader at the Department of Concrete Construction and Bridges.

Vladimír PRIECHODSKÝ
Civil Eng.
Techn. Univ.
Bratislava, Czechoslovakia

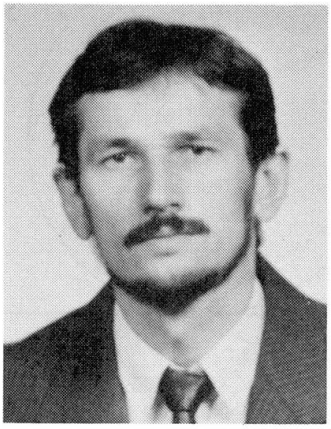

Vladimír Preichodský, born 1953, obtained his civil engineering degree at the Slovak Technical University Bratislava, where, he is currently working as a researcher at the Department of Concrete Construction and Bridges.

SUMMARY

A thick-walled concrete ring model is presented to analyze the state of stresses in the anchored zone of ordinary reinforcement and prestressing steel. The stress-strain diagram of concrete with an ascending and descending branch was used to describe the measured, large, relative strains. A gradual plastification starting from the internal surface of the ring towards the external one was observed.

RÉSUMÉ

Un modèle d'anneau en béton à parois épaisses est étudié en vue d'analyser l'état de contrainte régnant dans la zone d'ancrage d'armatures ordinaires et des aciers de précontrainte. Le diagramme contrainte-déformation du béton présentant une branche croissante et décroissante a été pris en compte lors de la description des déformations relatives élevées obtenues. Les résultats montrèrent une plastification progressive s'étendant de la face intérieure de l'anneau jusqu'à sa face extérieure.

ZUSAMMENFASSUNG

Es wird ein dickwandiges Betonring-Modell vorgestellt und zur Analyse der Spannungen im Eintragungsbereich der Bewehrungsstäbe und Spanndrahtlitzen herangezogen. Für die Beschreibung der gemessenen grossen örtlichen Dehnungen wird ein Kraft-Verformungs-Diagramm mit einem steigenden und einem fallenden Ast benützt. Es wurde eine kontinuierliche Plastifizierung des Querschnitts vom inneren zum äusseren Rand des Betonrings festgestellt.

1. INTRODUCTION

Anchorage of deformed bars and strands by bond causes relatively large radial compressive stresses at the interface between steel and concrete. A thick-walled concrete ring model has been considered to analyse the influence of radial compressive stress on the state of tensile stresses in the anchored area. The concrete ring approximates the effect of the surrounding concrete. The cylinder can be located in the beam section as shown in Fig. 1.

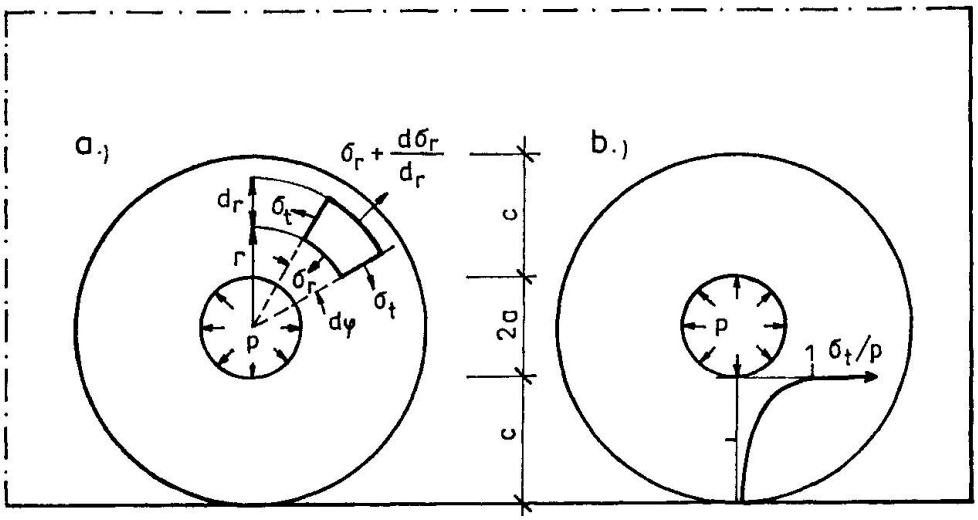

Fig. 1: a/ Location and geometry of the ring model in the section and stresses on an element.
b/ The variation in tangential tensile stresses in the ring model at the elastic stage.

The stresses are mostly calculated for an elastic or plastic stage:

- a solution for the stresses in a thick-walled ring subjected to internal pressure at the elastic stage is given by Timoshenko [1],
- the concrete is assumed to act plastically, that is the ring will not break until the stresses in the tangential direction at every part of the ring section have reached the ultimate tensile concrete stress [2].

2. EXPERIMENTAL TESTS FOR EVALUATION OF STRAINS

The variation in tangential and radial strains were investigated on thick-walled concrete rings with inner radius a = 9 mm, outer radius b = 50, 100, 150 mm and a height of 30 mm. The test rings concrete mix was of the following properties:

- the aggregate was a washed river sand with a maximum size of 4 mm,
- compressive cube strength $f_c = 37,9\ N.mm^{-2}$,
- tensile strength $f_t = 2,8\ N.mm^{-2}$,
- modulus of elasticity $E = 28\ 125\ N.mm^{-2}$ and Poissons ratio $\nu = 0,134$ at stress level of about 40 % of ultimate strength.

The rings were subjected to hydraulic pressure on the inner surface. The deformations of the rings were monitored with electric resistance strain gauges (length 8 mm) in the radial and tangential direction - see Fig. 2. The observed relative tangential strains ε_t and relative radial strains ε_r in the ring model for the increasing internal radial pressure p_i are plotted in the Fig. 2. In order to show the ability of the model to carry large strains it was importante to measure also the strains in the fracture zone, i. e. where the final failure occurs due to a crack.

3. TEST RESULTS AND DISCUSION

Fig. 2 shows that the tangential strains measured in the fracture zone are much higher (Fig. 2b) than that observed outside this zone (Fig. 2c, d, e).
Before the ring fails due to a crack in the fracture zone, under increasing radial pressure, a strain decrease was registrated outside the fracture zone. The following general conclusions regarding the experminental tests may be drawn:

1. The measured tangential strains in the fracture zone reached the maximal value $\varepsilon_t = 2,4.10^{-3}$ which many times exceeds the ultimate strain recorded at the centric tension test $\varepsilon_t = 0,12.10^{-3}$.
2. The test indicate that the observed maximum carrying capacity of the rings, exposed to internal radial pressure are lower than the theoretically carrying capacity at the plastic stage. These informations indicate that the intensity of tangential stress is considerably lower if the strain in the fracture zone exceeds a certain critical value. This fact shows that the fictitious crack model [3] gives a realistic description of tensile stresses in the tested rings. Based on the fictitious crack model it was possible to describe the state of tensile stresses in the ring.

The ascending branch of the stress-strain diagram was determined by means of the tensile test. The descending branch have been determined from the strains measured just before the final failure occurs and from the observed carrying capacity of the rings.
The carrying capacity is given by

$$\int_a^b \sigma \, dr = p.a \qquad (1)$$

The stress-strain diagrams of concrete for various inner radius are shown in Fig. 3.

Fig. 4 shows the variation in the tangential tensile stresses according to the stress-strain diagrams in Fig. 3.
It can be seen a continual transmission from elastic to elastoplastic stage starting from the internal surface of the ring towards the external one. From the distribution of the stresses it is evident that it is not possible to consider the ultimate tensile strength evenly distributed over the cross section.
The measured load capaties of the tested concrete rings, at the time cracks first appear, are plotted in Fig. 5. The experimental values occur just where expected, i. e. between the elastic and plastic stages.

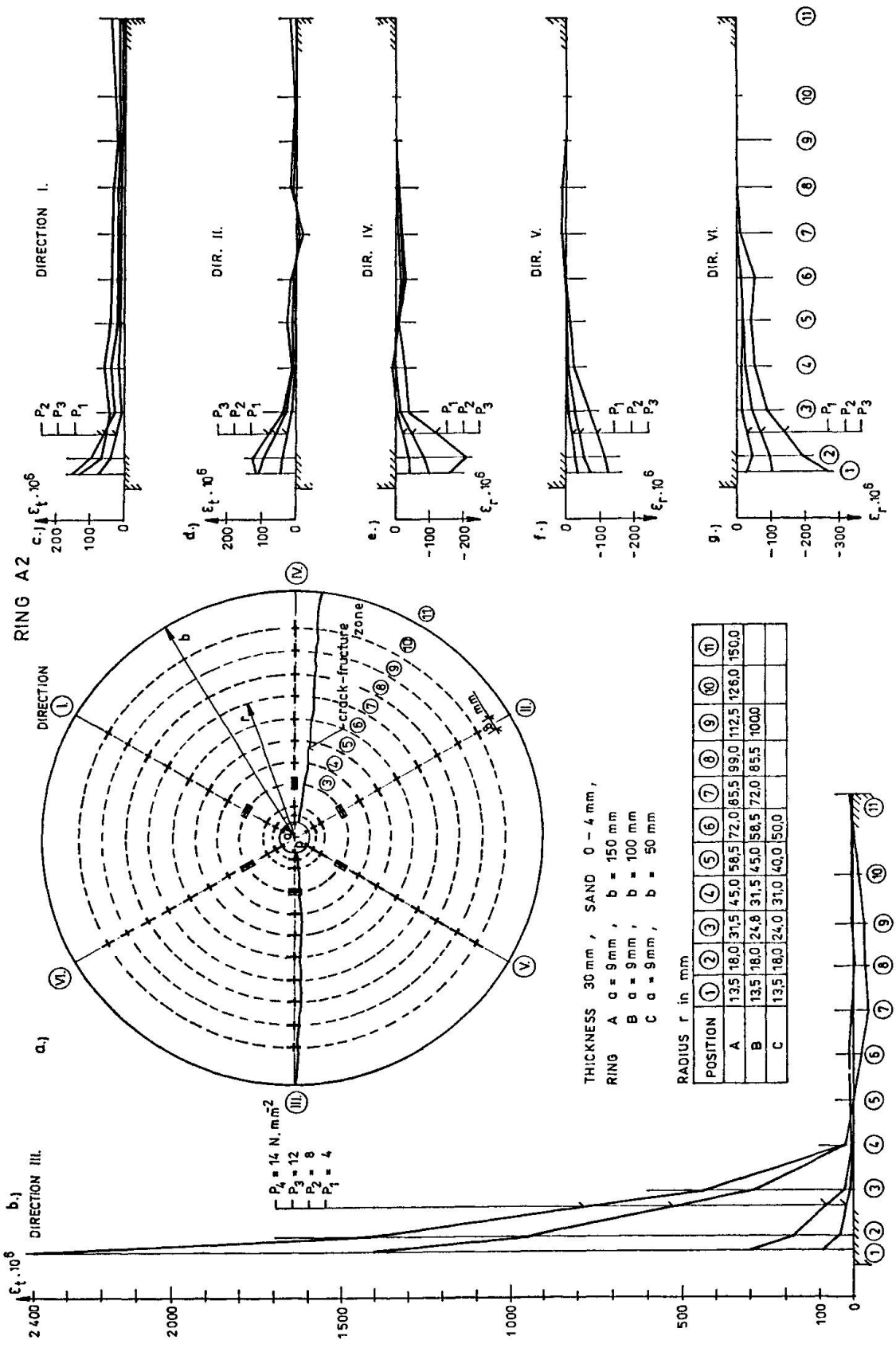

POSITION	①	②	③	④	⑤	⑥	⑦	⑧	⑨	⑩	⑪
A	13,5	18,0	31,5	45,0	58,5	72,0	85,5	99,0	112,5	126,0	150,0
B	13,5	18,0	24,8	31,5	45,0	58,5	72,0	85,5	100,0		
C	13,5	18,0	24,0	31,0	40,0	50,0					

Fig. 2: The variation in the relative strains ε_t and ε_r in the ring model

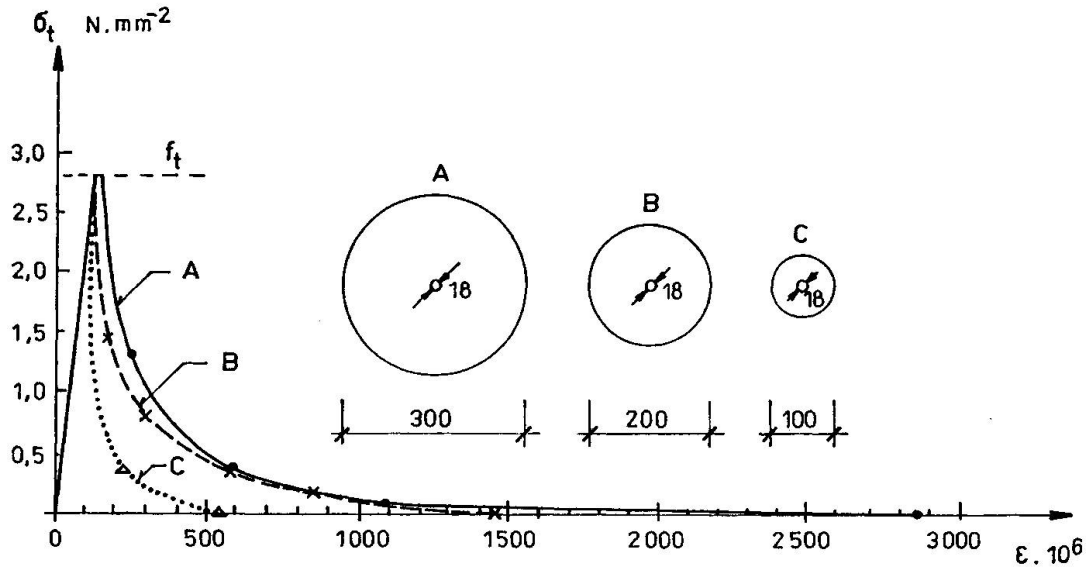

Fig. 3: Stress-strain diagrams of concrete in tension

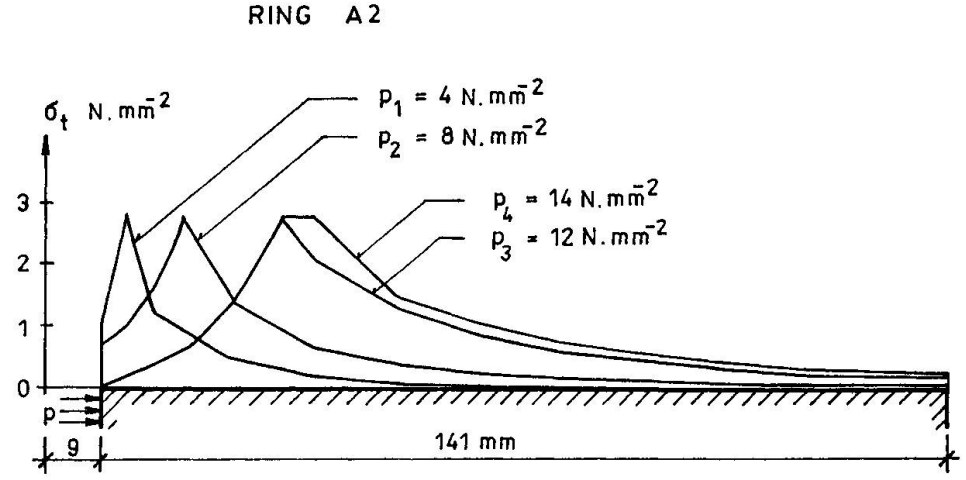

Fig. 4: The variation in the tangential tensile stresses for the increasing internal pressure

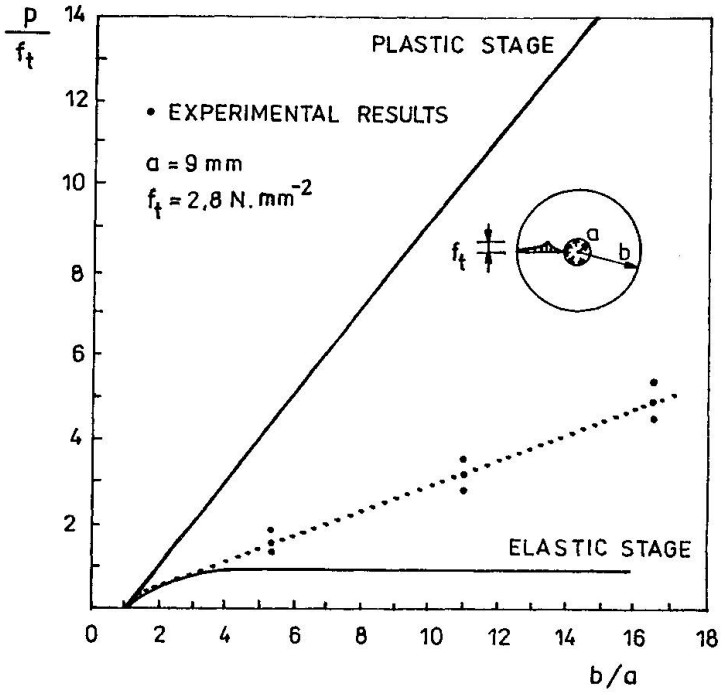

Fig. 5: Load carrying capacities of the rings on occurrence of cracking.

4. CONCLUSIONS

Realized tests confirm that by means of the elastoplastic ring model, based on the stress-strain diagram with an ascending and descending branch, it is possible to analyse the state of the tensile stresses in the transmission zone of prestressed or non-prestressed reinforcement. Futher tests based on the same approach are recomended in order to obtain valid results for practical design purposes.

REFERENCES

1. TIMOSHENKO S., Strength of materials Part II: Advanced theory and problems. Princeton, N.J.,D van Nostrand Company Inc. 1956. pp. 205-210.

2. TEPFERS R., A theory of bond applied to overlapped tensile reinforcement splices for deformed bars. Gothenburg, Chalmers University of Technology, Division of Concrete Structures, 1973, Publication 73:2.

3. HILLERBORG A., Reliance upon concrete tensile strength. IABSE Colloquium "Structural concrete", Stuttgart, April 1991.

4. KÖNIG G., DUDA H., Basic Concept for Using Concrete Tensile Strength, ibid.

5. KÖNIG G., SCHEIDLER D., FEHLING E., Grundlagen zur Traglast-ermittlung unbewehrter Betonbauteile unter Zugbeanspruchung, Beton und Stahlbetonbau, November 1986. pp. 292-296, December

Transverse Tension Decisive for Compressive Resistance of Concrete Cover

Importance de la tension transversale pour le résistance en compression du recouvrement de béton

Querzug massgebend für Mitwirkung der Betondeckung in der Druckzone

Walter STREIT
Res. Assist.
Techn. Univ. Munich
Munich, Germany

W. Streit, born in 1956, received his civil engineering degree at the University of Munich in 1981. For two years he was research assistant of Professor E. Grasser. After that he worked for one year at the construction company DYWIDAG. Since 1985 he is assistant of Professor Kupfer.

Jürgen FEIX
Res. Assist.
Techn. Univ. Munich
Munich, Germany

J. Feix, born in 1961, received his civil engineering degree at the University of Munich in 1986. After that he worked for one year at the construction company DYWIDAG. Since 1987 he his assistant of Professor Kupfer.

Herbert KUPFER
Prof. for Struct. Eng.
Techn. Univ. Munich
Munich, Germany

H. Kupfer, born in 1927, received his civil engineering degree at the University of Munich in 1949. For six years he was an assistant of Professor Rüsch. After that he worked at the construction company DYWIDAG, lattely as chief engineer. Since 1967 he is Full Professor for structural engineering at the above-mentioned university.

SUMMARY
To ensure the durability of reinforced concrete members, concrete cover has been increased lately. This paper shows that the strength of members may be reduced by an increasing concrete cover because this often leads to a higher transverse tension in the concrete cover of the compression zone, for example in frame corners subjected to positive moments and in beams subjected to shear and bending.

RÉSUMÉ
On montre qu'un accroissement du recouvrement de béton – pour des raisons de durabilité – peut entrainer une réduction de la résistance de certains membres du fait d'une augmentation de la tension transversale dans la zone de béton en compression. Cela peut ainsi réduire de façon notable la résistance à la rupture dans des angles soumis à des moments positifs.

ZUSAMMENFASSUNG
In diesem Beitrag wird aufgezeigt, dass die aus Gründen der Dauerhaftigkeit erhöhten Betondeckungen die Tragfähigkeit von Bauteilen negativ beeinflussen können, da die Vergrösserung der Betondeckung in vielen Fällen höhere Querzugbeanspruchungen in Betondruckzonen hervorruft. Dies gilt z.B. bei Rahmenecken mit an der Innenseite Zug erzeugender Biegebeanspruchung und bei Balken, die auf Schub und Biegung beansprucht sind.

1. INTRODUCTION

Concrete cover is usually regarded today as a perfect part of the compression zone. In general a sufficient tensile strength of concrete must be presupposed to do so.

A change of direction of the compressive stresses in frame corners subjected to positive moments as well as a change of magnitude of the compression force in beams with acting shear reinforcement causes tensile stresses in the concrete cover of the compression zone.

But all common codes allow omission of these tensile forces.

In the cases mentioned before a biaxial stress state exists. It must be considered that with increasing longitudinal compressive stress the transverse tensile strength is decreasing /1/. Our design rules were derived from laboratory tests, which were carried out with preciseness avoiding temperature shocks; therefore it is to be expected that in these tests the tensile strength was much higher than in practice. Furthermore most of these tests were made with a very thin concrete cover (1.0 - 2.5 cm), which is smaller than the concrete cover claimed by codes to ensure durability (Table 1).

Member	Exposure Class	DIN 1045 59	DIN 1045 72/78	DIN 1045 88	MC 78	MC 90	EC2 90	
Slabs	interior	10	10	20	15	20	20	[mm]
	humid	15	20	30	20	35	25	[mm]
	humid de-icing	<40	30	50	30	50	40	[mm]
Beams	interior	15	15	20	15	20	20	[mm]
	humid	20	25	35	25	35	30	[mm]
	humid de-icing	<40	35	50	35	50	45	[mm]

Table 1 Comparison of the concrete cover for different codes (nominal values)

In this paper some examples will show that the influences mentioned above can lead to safety risks even when the requirements of the codes are fulfilled.

2. FRAME CORNERS WITHOUT INCLINED REINFORCEMENT

Extensive laboratory tests of frame corners without inclined reinforcement subjected to positive moments were performed by Nilsson /2/ and Kordina /3,4/. Especially in cases of higher reinforcement ratios failure occured far below the calculated ultimate moment. The calculated ultimate moment was determined at an even beam for the same reinforcement. The reason for failure is generally a spalling of concrete cover or of the outer part of the compression zone in that area, where the compression force is being diverted. Afterwards the resisting

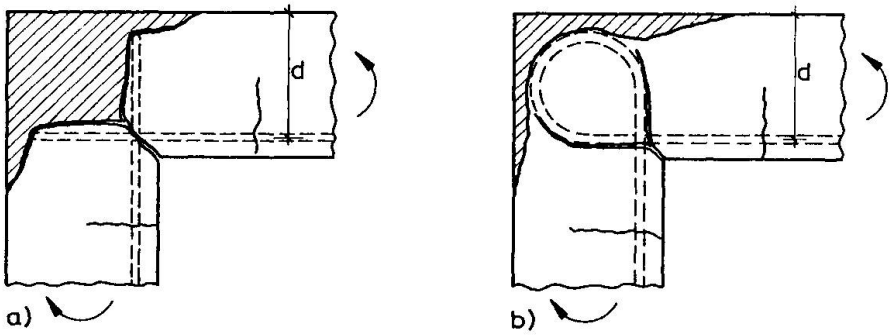

Fig. 1 Graphical illustration of the failure for two different tests of corners subjected to positive bending moments (and two different types of reinforcement)

moment decreases abruptly. Already under a small load a crack begins to form at the inside of the corner. Under higher load the crack divides into two cracks which approximately follow the reinforcement until the tensile force, which is necessary for diverting the compression force, cannot be carried any more and failure occurs. For example see the two crack patterns in Fig.1.

The force distribution in the corner can be described simplified by means of a strut and tie model /5/, which takes into account the failure mechanism and therefore separates the forces in the concrete cover /6/. See Fig.2.

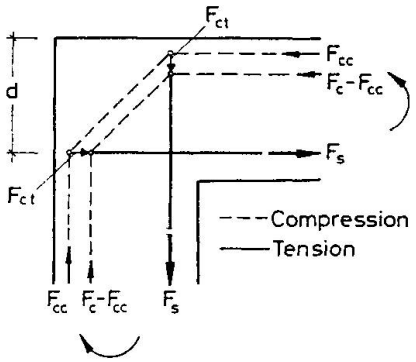

Fig. 2 Strut and tie model illustrating the failure mechanism.

This simple model shows that the compressive force F_{cc} of the concrete cover can only be diverted by the tensile Force F_{ct} resulting from concrete tensile stresses. The compressive force F_{cc} has to be determined with an area A_c, the height of which must exceed the concrete cover c, because the crack area between the reinforcement bars is curved (Fig.3). In this paper the area A_c is determined simplified by $A_c = b \cdot c' = b \cdot (c+s/4)$ with c = concrete cover and s = distance of the bars. The approximation s/4 means that the crack area assumed to be a parabolic area with a maximum inclination of 1.5:1.

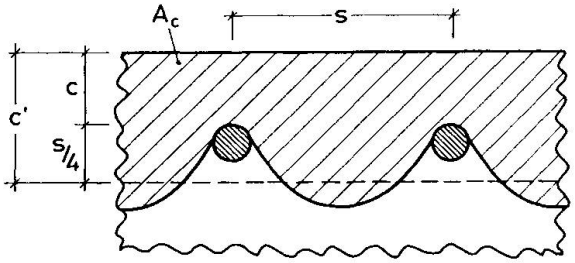

Fig. 3 Area A_c for the determination of the compression force F_{cc} of the concrete cover.

Taking into account the fast increasing of F_{cc} with increasing concrete cover for a given bending moment it is evident that also the tensile stresses which are decisive for the failure, grow fast. If in case of a small concrete cover the tensile strength is already utilized, it is obvious that in case of a larger concrete cover an equilibrium is only possible if a reduction of the bending moment occurs.

The German code DIN 1045 allows the design of frame corners subjected to positive bending moments without inclined reinforcement up to a reinforcement ratio $\mu = 0.4$ %. It must be pointed out, that a limitation of μ is not a good criterion but that a limitation of $\omega = \mu \cdot f_s/f_{ct}$ (a mechanical reinforcement ratio referred to the tensile strength of concrete) would be more precise.

In case of reinforcement ratios $\mu < 0.4$ % and normal concrete strength the influence of the concrete cover in the range of $2cm \leq c \leq 5cm$ at the compression

zone is without much importance for members with small depth ($d \leq 20$ cm), because the neutral axis depth x for the calculated ultimate moment is not much higher than c'(for c = 2 cm). But in case of members of intermediate height (d ~ 50 cm)the influence of the concrete cover (at the compression zone) on the resistance may be great.

Taking, for example, a member with μ = 0.4 %, B 35 (DIN 1045)$\cong$ C 30/37 (EC2), d = 40 cm and s = 8 cm, an increase of the concrete cover from c = 2 cm to c = 5 cm causes an increase of F_{cc} of about 25 %. Assuming that for a concrete cover c = 2 cm the resistance due to the transverse tension is already met, so that no greater F_{cc} can be carried, the failure moment is about 17.5 % lower. Taking into account the influence of the longitudinal compressive stress on the transverse tensile strength acc. to /1/ the failure moment is still about 10 % lower, because the longitudinal stress at the distance c' from the edge is decreasing with increasing c' (in case of a depth of d = 60 cm the failure moment is for c = 5 cm about 14 % lower than for c = 2 cm, taking the changing tensile strength into account). The ultimate moments calculated from a regular design for bending of the cross section remaining after spalling is for d = 40 cm lower than, and for d = 60 cm almost equal to the failure moment in case of the spalling of the concrete cover. That means that in cases of higher cross-sections the calculated ultimate moment at the face of the corner for the cross-section remaining after spalling is higher than the moment when the concrete cover spalls. But it is possible, too, that for high cross-sections the failure moment is lower than the calculated one of the remaining cross-section in the face of the corner, because of excessive damage of the corner area during spalling of the concrete cover (compare Fig.1a).

3. FRAME CORNERS WITH INCLINED REINFORCEMENT

Tests showed that the failure of frame corners with inclined reinforcement occurs in a different way from the failure of corners without inclined reinforcement /2,3/. Fig. 4 presents examples for typical failure in case of additional inclined reinforcement. Failure does not start anymore at the face of the corner as shown in Fig.1 but at the area of the anchoring of the inclined reinforcement. The reorientation of the compression force of the concrete cover already takes place in this area and the resulting transverse tension leads to failure. In cases of corners with inclined reinforcement the failure moment was usually greater than the calculated ultimate moment in the face of the corner (neglecting the inclined reinforcement). Tests were carried out only up to rein-

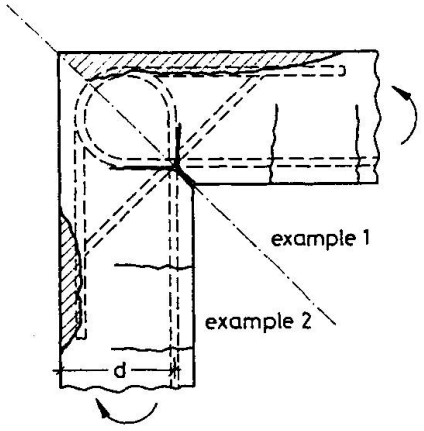

Fig. 4 Graphical illustration of failure of corners with inclined reinforcement subjected to positive bending moments

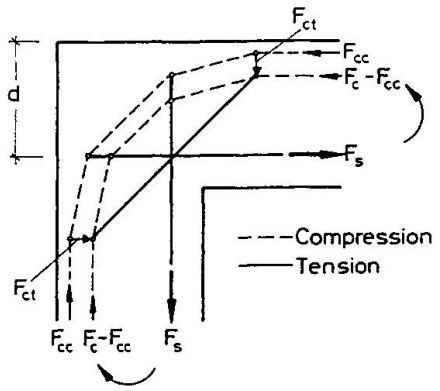

Fig.5 Strut and tie model, illustrating the failure mechanism

forcement ratios of μ = 1.1 %. All test specimen were reinforced in a way that failure should be initiated by flow of the reinforcement but it was observed in all tests that the failure was caused by spalling of the concrete cover in the area of the anchoring of the inclined reinforcement. The strain of the longitudinal reinforcement at failure amounted to about 2 ‰

A simplified strut and tie model presented in Fig.5 clearly shows the failure mechanism. The compression force F_{cc} of the concrete cover is already diverted in the area of the anchoring of the inclined reinforcement (activated for the sake of compatibility). The area of the face of the corner which is decisive for the failure of corners without inclined reinforcement, is relieved.

In the following the test V4 of Kordina is used as an example. The ratio of the failure moment to the calculated ultimate moment for pure bending was 1.0 (due to a normal force in tests the failure moment related to the axis of the tension reinforcement must be used). In the test specimen concrete cover was 2 cm. In case of a concrete cover of 5 cm the failure moment was calculated in accordance with chapter 2 by comparing the forces F_{cc}, in view of the influence of the compressive stress on the transverse tensile strength. The calculated ultimate load for the cross section remaining after spalling is of about the same size as the moment when the concrete cover spalls. The reinforcement ratio ot the test V4 was μ = 0.86 %. But the decisive value of μ corresponding to the compressive force $F_c < F_s$ is only μ = 0.76 %, because a tensile axial force was acting on the cross-section. When the reinforcement ratio is related to the tensile strength of concrete, it becomes evident that this test in relation to all other tests of /2,3/ is among the most reinforced ones.

Taking into account that the tensile strength in practice is usually lower than in laboratory tests it is to be expected that in practice failure moments are lower, too. In corners with inclined reinforcement failure moment will increase moderately with increasing reinforcement ratio, because the cross section, which remains after spalling of the concrete cover will become decisive provided that the compression zone in the corner is not damaged too much.

4. BEAMS SUBJECTED TO BENDING AND SHEAR

Along a beams with high shear there is a rapid change of the compressive force. This means that there is also a rapid change of the compressive force F_{cc} in concrete cover; for example see the area close to the point of zero moments (Fig. 6).

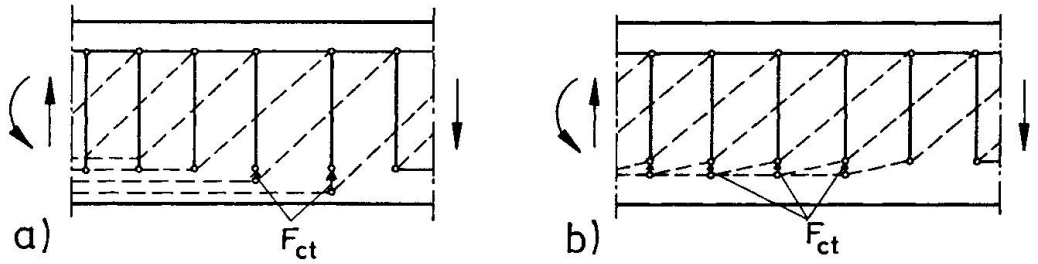

Fig. 6 Two Models illustrating a possible force distributions in a beam under high shear in the area close to the point of zero moments.

The model in Fig. 6a produces in case of thick concrete cover average transverse tensile stresses $\sigma_{ct} = \tau$. Further on it will be shown that the model in Fig.6b causes smaller tensile stresses.

The force distribution in the compression zone for model Fig. 6b was examined for different concrete covers computing the compression zone as a wall. The influence of the thickness of the concrete cover was examined for the most unfavourable case of a beam with a overall depth of 30 cm (effective depth of 25 cm) and with a compression zone heigth of 10 cm. The compression field was

supposed to act under an angle of 45^0 and to be uniformly distributed along the upper rim of the wall. The spacing of the stirrups was assumed to be 10 cm. Furthermore it was supposed that the transmission of the stirrup force into the wall-segment should cause constant forces along the length x-c", where c" = c + ϕ_s = c + 1 cm. Linear and constant distribution of the compressive stresses were examined, the resulting transverse tensile stresses differed only slightly. All calculations are based on a linear elastic behaviour of the material. For a concrete cover of c = 1 cm (c"= 2 cm) the average tensile stress amounts to about 9 % of the assumed acting shear stress τ. For a thick concrete cover c = 5 cm (c" = 6 cm) the calculation showed destinctly higher average tensile stresses of even more than 40 % of τ. Localized tensile stresses are even considerable higher.

This simplifying analysis shows that beams with a thick concrete cover which are substantially subjected to shear may reach an ultimate limit state by a spalling of the concrete cover. To what extent these theoretical results are representing the actual behaviour in the concrete cover should be checked by future tests.

5. SUMMARY

This paper deals with the negative influence of the increase of concrete cover upon the resistance of reinforced concrete. In codes the concrete cover was enlarged in the sake of the durability of concrete structures.

The influence of an increase of concrete cover on the transverse tensile stresses was examined in the case of a corner (with and without inclined reinforcement) subjected to positive bending moments. It was shown theoretically that an increase of concrete cover often leads to a substantial increase of the transverse tensile stresses in concrete. This causes also a substantial decrease of the failure moment compared with members with smaller concrete cover.

Also in cases of beams with high shear the transverse tensile stresses in the concrete cover of the compression zone increases considerably with increasing concrete cover.

The authors think that experimental research is urgently necessary to clarify the negative influence of an increasing concrete cover on the resistance of reinforced concrete.

REFERENCES

1. Kupfer H.B., Das Verhalten des Betons unter mehrachsiger Kurzzeitbelastung unter besonderer Berücksichtigung der zweiachsigen Beanspruchung. Deutscher Ausschuß für Stahlbeton, Heft 229, Verlag Ernst & Sohn, Berlin 1973

2. Nilsson I.H.E., Reinforced concrete corners and joints subjected to bendcing moments. Document D7, 1973, National Swedish Building Research, Stockholm 1973

3. Kordina K., Bewehrungsführung in Ecken und Rahmenknoten. Deutscher Ausschuß für Stahlbeton, Heft 354, Verlag Ernst & Sohn, Berlin 1984

4. Kordina K., Fuchs G., Untersuchungen zur Anwendung von hakenförmigen Übergreifungsstößen in Rahmenecken. Vorläufiger Abschlußbericht, Technische Universität Braunschweig 1970

5. Schlaich G., Schäfer K., Konstruieren im Stahlbetonbau. In: Beton-Kalender 1989, Teil 2, Verlag Ernst & Sohn, Berlin 1989

6. Breen J.E., Why structural concrete. Introductors Report, IABSE Colloquium "Structural Concrete" 1991 Stuttgart

Dimensioning of Elements with Built Up Steel Corbel at the End

Dimensionnement d'éléments en béton munis de cornières métalliques à leur extrémité

Bemessung am Auflager als Stahlkonsole ausgebildeter Elementen

József ALMÁSI
Assoc. Prof.
Techn. Univ.
Budapest, Hungary

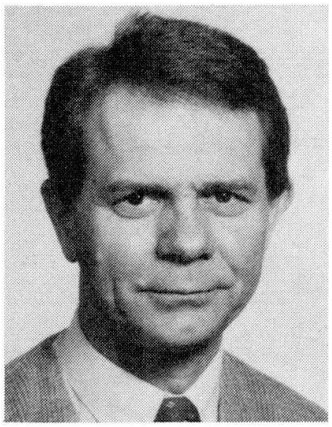

József Almási, born 1940, received his civil engineering degree at the University of Budapest in 1964, and Ph.D. degree in 1972. The focus of his work nowadays is plasticity and detailing.

SUMMARY

The paper reviews experimental work on specially supported elements, where there is discontinuity in geometry and load. It proposes three calculation models: crack free state, cracked state, and strut-and-tie. The determined tensile forces can be followed with a good detailed reinforcement fulfilling the serviceability limit state requirements.

RÉSUMÉ

L'article présente le travail expérimental effectué sur des éléments sur appuis spéciaux, où l'on a constaté des discontinuités dans la charge et la géométrie. Trois méthodes de calcul sont proposées: état non-fissuré, fissuré et analogie du treillis. Les forces de traction calculées peuvent être requises par une armature détaillée assurant les conditions de l'état limite de service.

ZUSAMMENFASSUNG

Der Aufsatz gibt einen Überblick über Versuche besonders gelagerter Träger, bei denen in Geometrie- und Belastung-Diskontinuitäten vorkommen. Drei Berechnungs-Methoden werden vorgeschlagen: Rissefreier Zustand, Riss-Zustand, und Stabwerk-Modell. Die berechneten Zugkräfte können mit Bewehrung abgedeckt werden, die die geforderten Ansprüche hinsichtlich Gebrauchstauglichkeit erfüllt.

1. INTRODUCTION

Structural elements can be used for various purposes if their supporting is solved in an "adjustable" way at the butt end. This is shown in Fig.1 e.g. on a floor-plate element, where on the left side the built up steel corbel has a lower- and on the right side an upper position.

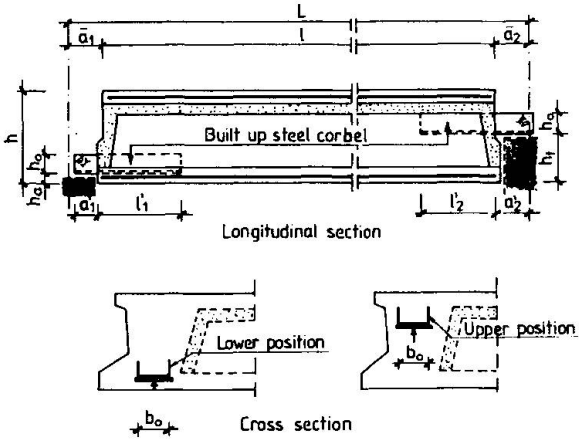

Fig.1 Floor plate element with built up steel corbel at the end

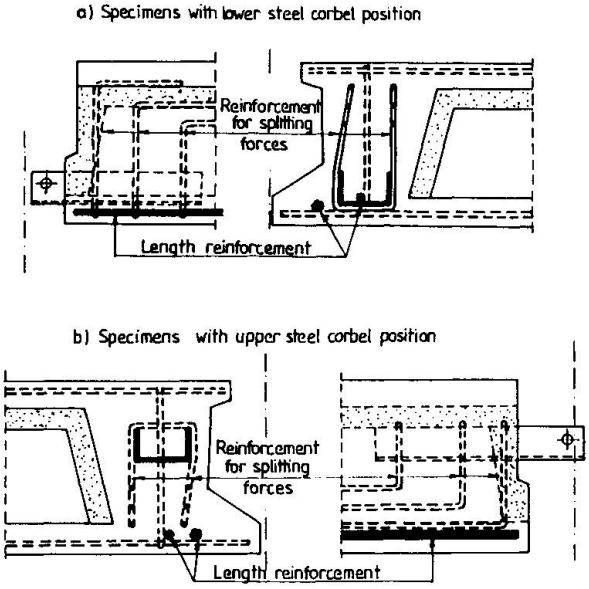

Fig.2 Reinforcement at the support for the specimens

The paper reviews some dimensioning methods which can be used at the support, considering concrete tensile strength 1,2 .

2. RESULTS FROM THE EXPERIMENTAL WORK 7

The reinforcement of specimens for the test is shown in Fig.2. During the step-by-step loading we measured the concrete surface strains and crack width. The typical crack patterns are shown in Fig.3 and 4.

With the steel corbel in the lower position it was found that the concrete surface around the corbel was crack free until 75% of the ultimate load. The cracks started from the inside-end of steel corbel. These craks can be regarded as splitting craks. Generally at the same load level bending cracks can also be found.

In the specimens where the steel corbel was in upper position we found crack free state until 60% of the ultimate load. The cracks started from the butt-surface, from the corner of steel corbel ascend.

In both cases the failure was caused by the yielding of vertical reinforcement.

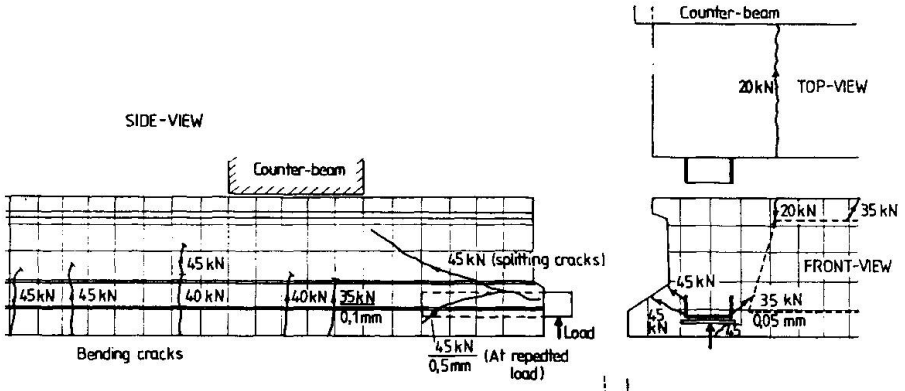

Crack patterns at „lower" position of built up steel corbel

Fig. 3.

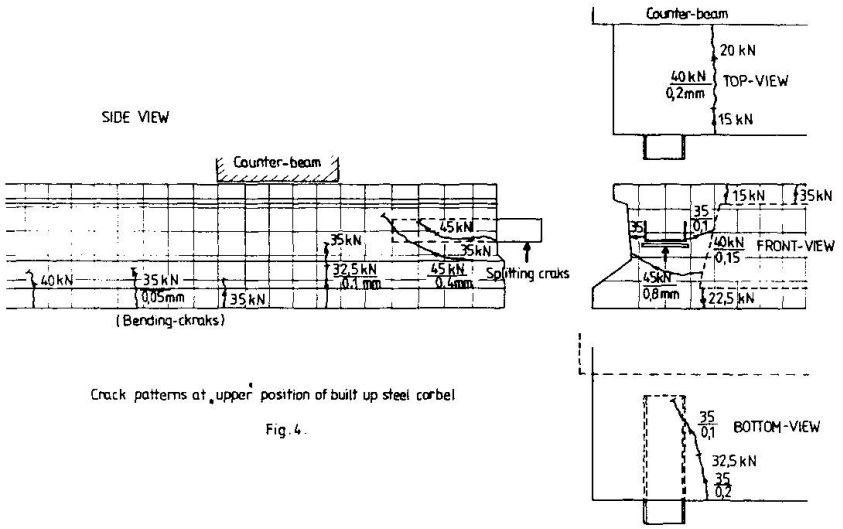

Crack patterns at „upper" position of built up steel corbel

Fig. 4.

3. POINT OF VIEWS OF DIMENSIONING

Besides providing ultimate limit state and serviceability limit state requirements during the dimensioning we have to take into account the following:

The steeel corbel outstanding from the concrete should be stiff in order to have a very small deflection. The sufficient built up length l_1, l_2 Fig.1 of steel corbel has to be provided.

A possible failure can cause a large economic damage and has a significant danger for the human life, therefore at the dimensioning we cannot take directly into account the tensile strength of concrete, because of brittleness 1,2 . Splitting forces arising around the steel corbel can be counterbalanced with vertically placed reinforcement Fig.2, where we can use one admissible value of tensile strength for concrete at the anchorages.

At the detailing we have to be ensure the connection between the steel corbel and the longitudinal reinforcement of the element, and to enlarge the redistribution zone by use of vertical reinforcement 2 . For the calculation of forces around the steel corbel we can use different types of models.

4. MODELS FOR CALCULATION

In this chapter we suggest some calculation models. We assume according Sant-Venant principle that part of the whole element near the support can be regarded like an independent structure.

4.1 Crack free state

Based on the experimental results 7 we assumed three typical, crack patterns Fig.5. where cracks are concentrated in one place. Along the fully developed cracks the tension stress distribution was taken from fracture mechanics approaches. The failure occurs if tensile stresses in concrete arrive the tensile strength f_t. The calculated tensile force is $F_{cr} = b \cdot \sum A_\sigma$. Reinforcement calculated from the vertical component helps to avoid brittle fracture. If the steel stress is reduced appropriately (exp. $\sigma_s = 0{,}4 \cdot f_{sy}$) the crack width can be controlled. By distributing reinforcement according to the tensile stresses, we can fulfilled the requirements (s.Ch.3.).

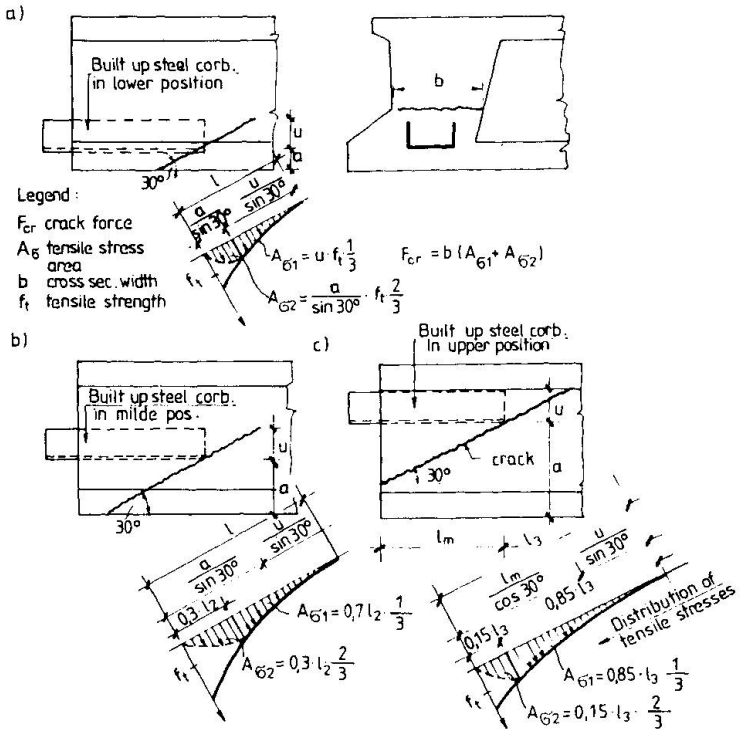

Fig.5 Calculation models in crack free state

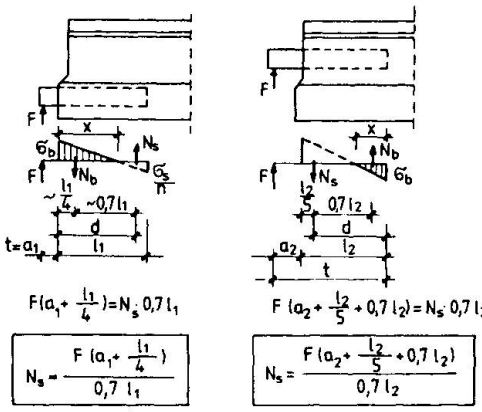

Simplified calculation of the tensile forces

Fig.6

4.2 Cracked state

In the cracked state the equilibrium is arrived through reinforcement. A simplified calculation model is shown in Fig.6 . To use the moment equilibrium we have to choose some geometrical dates in the right way, or to make the traditional calculation. To fulfill the serviceability limit state requirements controll of the crack width, through the stresses in the tensioned members N_s has to be carried out.

4.3 Strut-and-tie models

To have clear "detailing" rules we need a more accurate model like strut-and-tie 5 . Depending on the position of the steel corbel we can develop three typical strut-and-tie models Fig.7 which follow the force paths indicated by the theory of elasticity. Controll calculation showed that strut-and-tie elements can be built up from concrete combining them with elements from the steel corbel, instead of using the steel corbel as a stiff body in this system. The results of an elastic calculation are given in Fig.7. The bearing capacity of concrete compression struts are shownd in 3. Tie forces are counterbalanced with reinforcement Fig.2.

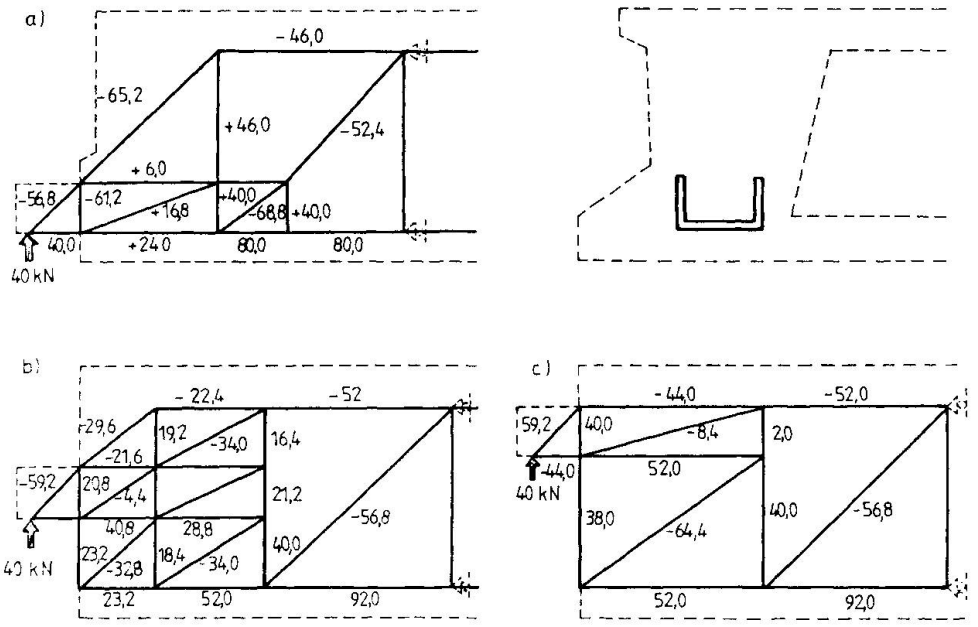

Fig.7 Strut-and-tie forces calculated on truss-construction

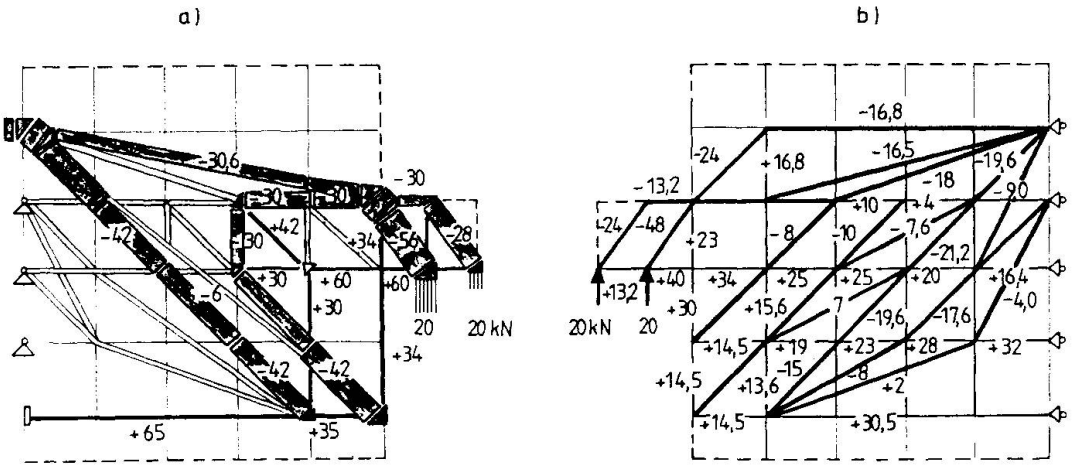

Calculation with stress fields

Fig.8

Calculation on detailed truss

If we chose a more detailed strut-and-tie model Fig.8b we get a finer force-distribution. Comparing these results with a more sophisticated calculation Fig.8a (statically admissible stress-field 6), we can find some differences in the forces. The clearly determined tensile forces followed with a proper detailed reinforcement, using one admissible tensile strength at the anchorages, secure us a good result.

References

1. HILLEBORG A., Reliance upon concrete tensile strength. In this report, IABSE Colloq. Stuttgart 1991.
2. KÖNIG G., DUDA H., Basic concept for using concrete tensile strength. In this report, IABSE Colloq. Stuttgart 1991.
3. WALRAVEN J.C., LEHWALTER N., Die Tragfähigkeit von Betondruckstreben in Fachwerkmodellen am Beispielen von gedrungenen Balken. Bet.u. Stahl. 84 (1989), H.4.
4. CLARK L.A., THOROGOOD P., Serviceability behaviour of reinforced concrete half joints. The Struc.Eng.No 18/20 Sept. 1988.
5. SCHLAICH J. Non-linear design on the basis of strut-and-tie models, FIP Symp. Israel, 1988.
6. SCHLAICH M., Computerunterstuzte Bemessung von Stahlbeton-scheiben mit Fachwerkmodellen. Professur für Informatik, ETH ZÜRICH, Bericht Nr. 1., 1989.
7. ALMÁSI. J. The behaviour of prefabricated elements with built up steel corbel at the end. Research Report VI.Techn. Uni. Budapest, Dep. of R.C., 1987 (in Hungarian)

Tensile Strength Concrete: Prodigal Son or Primary Source?

Résistance à la traction du béton: qu'en est-il?

Die Zugfestigkeit des Betons: verlorener Sohn oder Urquelle?

Andor WINDISCH
Civil Engineer
Dyckerhoff & Widmann AG
Munich, Germany

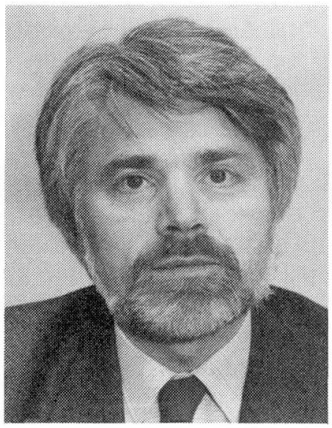

Andor Windisch, born 1942, obtained his Dr. techn. degree at the TU Budapest, Hungary in 1975. He served there as Assistant Professor for reinforced concrete structures until 1983. For 3 years he was Research Assistant at TU Stuttgart. He joined the R & D Department of a building company in 1987.

SUMMARY

Based on results of fracture mechanics and numerical modelling of concrete, the important role of the tensile strength as material property is discussed. The contribution shows that a) contrary to popular opinion high-strength concretes have a relatively high compressive strength compared to their tensile strength, b) the conditions in a structural concrete structure can be better characterized with a tension rather than a compression field, c) tensile strength of concrete must become an integral part of any physical model, d) tensile tests and not compressive tests should be applied in Quality Assurance.

RÉSUMÉ

Tout en se référant aux résultats donnés par la mécanique de la rupture et à la simulation numérique du béton, on discute du rôle primondial de la résistance à la traction du béton par rapport à la résistance en compression. Ce rapport met en valeur quatre aspects: a) Contrairement à ce que l'on pourrait penser, dans un béton à haute résistance, la forte résistance en compression ne va pas de pair avec la résistance en traction mobilisable. b) Les conditions régnant dans une structure en béton armé peuvent mieux être caractérisées par un champ de tractions que par un champ de compressions. c) Le résistance à la traction du béton doit devenir partie intégrante de tout modèle physique. d) Dans tout contôle de qualité, on devrait donner la priorité au test de résistance à la traction par rapport au test de résistance en compression.

ZUSAMMENFASSUNG

Bezugnehmend auf Ergebnisse, die bei Anwendung der Bruchmechanik und numerischen Modellierung zur Erforschung des Betons entstanden, wird die zentrale Bedeutung der Betonfestigkeit hervorgehoben. Der Beitrag zeigt, dass a) im Gegensatz zur allgemeinen Auffassung, die hochfesten Betone eine höhere Druckfestigkeit in bezug auf ihre Zugfestigkeit aufweisen, b) der Beanspruchungszustand eines Tragwerks aus konstruktivem Beton kann besser mit einem Zugfeld als mit einem Druckfeld beschrieben werden, c) die Zugfestigkeit muss als ein wichtiger Bestandteil aller physikalisch integeren Modelle betrachtet werden, d) die Qualitätskontrolle sollte statt die Druckfestigkeit, die Zugfestigkeit des Betons prüfen.

1. INTRODUCTION

Concrete is a inhomogeneous building material. It has a considerable and reliable compressive strength and a relative law tensile strength which can be even exhausted locally under unfortunate conditions, e.g. due to the hydration heat of cement or to its plastic shrinkage. It is quite obvious that the concrete tensile strength was always reprehended as the most unreliable concrete property.

As the compressive strength of the conventional test specimens (200 mm cubes or 150/300 mm cylinders) was rather insensitive to most of the aforementioned influences and it was convenient to be measured, it became accepted by the material science, the design office and the construction site as the fundamental mechanical property of concrete.

Several other properties were deduced empirically by the help of best–fit formulas using the compressive strength as basic variable.

The mean and fractile values of the different tensile strengths too became a function of compressive strength [1]. The degressive character (e. g. the fractional exponent) of this function reflects that high strength concretes have a relative lower tensile strength compared to low strength concretes. Obviously high strength concretes has been always treated as less perfect concretes.

According to a sad terminology, students learn to neglect the concrete tensile strength at dimensioning any s. c. member. Even the CEB–FIP Model Code [2] uses this verb, in EC 2 [3] the tensile strength will be ignored. (As a matter of fact, this applies to dimension the flexural reinforcement only.) In dimensioning of watertight or prestressed concrete members the tensile strength will be relied on with a shy consciousness of guilt.

Even quite recent engineering models for s. c. try to circumscribe those phenomena (e. g. bond) where the tensile strength is the main influencing factor. Thus the modeling of a slab without shear reinforcement became a quite unsolvable problem.

All these problems could be easily removed if we realize that the tensile strength is a more fundamental mechanical property of concrete as the compressive strength is.

The introduction of fracture mechanics and numerical modeling to describe the fundamental behaviour of concrete provides the chance to understand it and to rectify the hierarchy between tensile and compressive strength.

This paper intends to contribute to the acceptance of the tensile strength as a more fundamental concrete property.

2. COMPRESSIVE STRENGTH VS. TENSILE STRENGTH OR VICE VERSA

At the early seventies texture–oriented material models were developed to investigate the mechanism of the internal load bearing system of the two–phase composite material concrete [4], [5]. These models yielded qualitative and partly quantitative predictions on the load bearing and failure mechanisms as function of the rigidity– and strength–relationships between the cement matrix and aggregates. It was concluded that the characteristics of the interface between matrix and aggregate are the primary source of the mechanical properties. Depending on the differences in the rigidities of matrix and aggregates resp. the load trajectories are forced to local deviations in their course shich cause tensile stresses in the matrix and on the interface. These result in microcracks and inelastic response of the concrete. The microcracks were detected during compression tests [6].

During development of their model for "numerical concrete" Wittmann et al. [7] too realized the important influence of the interface on behaviour of concrete, the "mesolevel model" has been introduced.

The texture–oriented and the numerical models resp. showed that both, the compressive and tensile strength have the same origin: the adhesion of the matrix to the aggregates. Under tensile conditions the interface is stressed directly, under compressive conditions indirectly. In this latter case some internal redistribution in the load bearing system is possible, this is the source of the toughness of concrete under compression.

As methods of fracture mechanics had been applied to investigate concrete, it was not by chance that tensile and flexural tests were applied to determine the fracture energy, e. g. the fundamental characteristic of the material concrete, and not any compression test.

Thus we may hope that the traditional empirical way, how to deduce the tensile strength from the compressive strength will be converted to a physically right relationship: the compressive strength will be deduced from the tensile strength and the fractional exponent will disappear as well.

This would become an important step towards more reliance upon concrete tensile strength.

3. COMMENTS ON THE RELATIVE LOW TENSILE STRENGTH OF HIGH STRENGTH CONCRETES

The most important differences between the texture of a high strength concrete and a low strength concrete resp. are the higher stiffness and strength of the cement matrix and its higher adhesive strength to the aggregates in high strength concretes. Due to the quite similar stiffnesses of matrix and aggregate in high strength concretes the inner trajectories under compressive loading conditions are not forced to stronger local deviations, hence the induced stresses along the interface remain relative small. This results in a higher compressive strength compared to the given adhesive strength of the interface.

Thus a high strength concrete must not be reprehended any more for its relative low tensile strength but should be praised for its relative high compressive strength.

This would be an other step to recognition of the tensile strength.

4. COMPRESSION FIELD OR TENSION FIELD?

Soil has, similar to concrete, a low tensile strength compared to its compressive strength. The experts of soil mechanics continued to check form, position and load bearing capacity of sliding surfaces in soil structures even after introduction of the theory of plasticity.

Similar to soil structures, the condition of s. c. members can be better described with a tension field than with a compression field, unless the member will become over–reinforced,

The condition in different parts of a s. c. member can be characterized in relation to the probability of exceeding a certain fractile value of the tensile strength (f_{ctk}) in serviceability and ultimate limit states resp. This probability determines the necessary steps of dimensioning and the type of reinforcement to be applied:

- regions which probably remain free of cracks in ULS get minimum reinforcement
- regions where f_{ctk} will be exceeded in ULS, but probably not in SLS, must be reinforced without fulfilling the requirements in SLS. (As upto the ULS the tensile strength has been already exhausted, it can not be taken into account – instead of to be neglected or ignored – at fulfilling of equilibrium conditions. The usage of the verbs "neglect" or "ignore" is not correct.)
- regions where f_{ctk} has been exceeded already in SLS, the requirements both in ULS and SLS must be fulfilled as well.

This classification can not be achieved with any classes of effective compressive strengths of any compression field theory. Here once more the superiority of the tensile strength over compressive strength is highlighted.

5. BIAXIAL STRENGTH OF COMPRESSIVE STRUTS

Theory, experiments and practice prove that the concrete can be loaded bi– and triaxially, it has strengths in all directions [8].

The rapid decrease of the compressive strength under influence of transversal tensile stresses should not merely be considered at reduction of the axial strength of some compression elements in engineering models, but even the transversal tensile load bearing capacity of those compression elements which are not stressed upto the uniaxial prism strength should be realized as well.

According to the assumed strain distribution in the compression zone at ULS in flexure, only the most exterior concrete fiber reaches the compressive failure strain, all others have $\epsilon_c < \epsilon_{cu}$. This means that the load bearing capacity of any compression zone has a reliable transversal component as well, which is, as a matter of fact, the main part of the V_c term [9].

In ULS each fiber of the compression zone in a s. c. member with bending and shear, will fulfil the failure criterion simultaneously, the whole compression zone will fail at the same time. This was experienced and interpreted as the brittle character of the compression zone's failure under shear loading. The transversal stresses in the compression zone can be decreased with a transversal (shear) reinforcement but they can not be eliminated. Compatibility conditions will determine the effective ratio between V_c and V_s.

Accepting the biaxial strength of concrete some interpretation problems of recent engineering models [10], e. g.

- the shear strength of shear–unreinforced slabs
- the increase of the shear strength due to prestressing

would vanish immediately.

6. QUALITY ASSURANCE WITH TENSILE TESTS ON SITE

Performance and durability aspects have revealed the importance of concrete curing. The tensile strength is more sensitive to mistakes during curing as the compressive strength is.

In previous clauses the central part of tensile strength as concrete property has been discussed.

All these circumstances can leed to the conclusion that the quality control of s. c. structures should be performed with tension tests on the structure on site and not with compression tests on cubes or cylinders in the laboratory.

7. SOME COMMENTS ON THE INVITED LECTURES

7.1 Comments on the Test Setups

It is beyond any dispute that the uniaxial tension test is the most direct way to determine a strain–softening diagram. As it is difficult to carry out uniaxial tension tests on concrete under strain–controlled conditions, simpler test setups have been looked for and applied.

In order to achieve simply interpretable test results, test specimens with predetermined failure surfaces, e. g. notched beams in three point bending tests have been proposed as RILEM Recommandation [11]. It must be kept in mind that the predetermined failure surfaces do not yield that fractile value of G_F, which will govern the failure characteristics of a given

test specimen, as it will fail along its "weakest" surface, with the lowest G_F.

The specimen's form and the boundary conditions of that test, shich should yield more understanding about the fundamental properties of concrete need and must not be the simplest one, otherwise we shall have the same situation as with the compressive strength: we shall order and evaluate using an argument only for the reason that it is simple to be determined. It must be cleared up, which of the properties belong to the test setup, the specimen's behaviour and the material behaviour resp. as proposed in [13].

7.2 Comments on the Properties of the Fracture Energy

Fracture energy must be unique and independent of specimen type, size and shape. Size effect laws are felt to be created using the nominal stress

$$\sigma_N = P / (b \cdot d)$$

at evaluation of test results. These laws could be eliminated if the effective depth d_{ef} would be applied at evaluation of test results. The effective depth is that part of the specimen's depth, which is activated when the fictitious crack has first even came up to its maximum width (w_2). It is felt, that even the apparent dependence of the specific fracture energy with increasing ligament length could be eliminated using d_{ef}.

If it is true, that fracture energy is a material property, which has no direct connection with other material properties, such as the compressive strength [12], then we should look for more fundamental material properties, as after all, concrete is a quite simple composite, consisting of a porous matrix, aggregates and an interface between them. Nevertheless, as the influencing factors are the same as for the other mechanical properties [13], we will soon have a quite complete and coherent understanding for these properties and their relations.

REFERENCES

1. RÜSCH H., Die Ableitung der charakteristischen Werte der Betonzugfestigkeit. Beton 1955
2. CEB–FIP Model Code for concrete structures, 1978
3. Eurocode No. 2 Design of Concrete Structures. Final Draft 1989
4. WISCHERS G., LUSCHE M., Einfluß der inneren Spannungsverteilung auf das Tragverhalten von druckbeanspruchtem Normal– und Leichtbeton. Beton 1972
5. MODEER M., A Fracture Mechanics Approach to Failure of Concrete Material. Lund 1979
6. RÜSCH H., Physikalische Fragen der Betonprüfung. Zement–Kalk–Gips. 1959 Heft 1
7. WITTMANN F.H., ROELFSTRA P.E., KAMP C.L., Drying of Concrete – An Application of the 3L–Approach. Nuclear Engineering and Design. 1987
8. KUPFER H., Das Verhalten des Betons unter mehrachsiger Kurzzeitbelastung unter besonderer Berücksichtigung der zweiachsigen Beanspruchung. DAfStb. Heft 229, 1973
9. WALTHER R., Über die Berechnung der Schubtragfähigkeit...Beton– und Stahlb. 1962
10. MACGREGOR J.G., Dimensioning and Detailing. Invited Lecture Sub–theme 2.4
11. RILEM, Determination of the Fracture Energy of Mortar and Concrete by Means of Three–Point Bend Tests on Notched Beams. Materials and Structures 1985
12. HILLERBORG A., Reliance upon Concrete Tensile Strength. Invited Lecture 2.5
13. KÖNIG G., DUDA H., Basic Concept for Using Concrete Tensile Strength. Invited Lecture Sub–theme 2.5

Leere Seite
Blank page
Page vide